Weierstraß-Institut
für Angewandte Analysis und Stochastik

Leibniz-Institut im Forschungsverbund Berlin e. V.

Preprint ISSN 2198-5855

A porous-media model for reactive fluid-rock interaction in a dehydrating rock

Andrea Zafferi[1], Konstantin Huber[2], Dirk Peschka[3],

Johannes Vrijmoed[2], Timm John[2], Marita Thomas[1,3]

submitted: March 21, 2023

[1] Freie Universität Berlin
Department of Mathematics
and Computer Science
Arnimalle 9
14195 Berlin
Germany
E-Mail: andrea.zafferi@fu-berlin.de
marita.thomas@fu-berlin.de

[2] Freie Universität Berlin
Department of Earth Sciences
Malteserstr. 74-100
12249 Berlin
Germany
E-Mail: konstantin.huber@fu-berlin.de
j.c.vrijmoed@fu-berlin.de
timm.john@fu-berlin.de

[3] Weierstrass Institute
Mohrenstr. 39
10117 Berlin
Germany
E-Mail: dirk.peschka@wias-berlin.de
marita.thomas@wias-berlin.de

No. 2999

Berlin 2023

2020 *Mathematics Subject Classification.* 35D30, 35Q35, 37K58, 76Nxx, 76M30, 80A32, 80M30.

Key words and phrases. Reactive porous media, thermomechanical modeling, GENERIC, Darcy flow, equilibration of fast dissipative processes, time-discrete scheme.

AZ, KH, JV, TJ, and MT gratefully acknowledge the funding by the DFG-Collaborative Research Centre 1114 *Scaling cascades in complex systems*, project # 235221301, C09 *Dynamics of rock dehydration on multiple scales.* DP gratefully acknowledges the funding by the DFG-Priority Programme 2171 *Dynamic Wetting of Flexible, Adaptive, and Switchable Substrates* by project # 422792530. DP and MT also thank the Berlin Mathematics Research Center MATH+ and the Einstein Foundation Berlin for the financial support within the Thematic Einstein Semester *Energy-based mathematical methods for reactive multiphase flows* and by project AA2-9.

Edited by
Weierstraß-Institut für Angewandte Analysis und Stochastik (WIAS)
Leibniz-Institut im Forschungsverbund Berlin e. V.
Mohrenstraße 39
10117 Berlin
Germany

Fax: +49 30 20372-303
E-Mail: preprint@wias-berlin.de
World Wide Web: http://www.wias-berlin.de/

A porous-media model for reactive fluid-rock interaction in a dehydrating rock

Andrea Zafferi, Konstantin Huber, Dirk Peschka,
Johannes Vrijmoed, Timm John, Marita Thomas

Abstract

We study the GENERIC structure of models for reactive two-phase flows and their connection to a porous-media model for reactive fluid-rock interaction used in Geosciences. For this we discuss the equilibration of fast dissipative processes in the GENERIC framework. Mathematical properties of the porous-media model and first results on its mathematical analysis are provided. The mathematical assumptions imposed for the analysis are critically validated with the thermodynamical rock data sets.

1 Introduction

During its journey towards the subduction zone, the oceanic lithosphere cools and becomes hydrated, so that the fluid is chemically bound in solid phases. During subduction into the earth mantle, in turn, the plates heat up and the hydrous minerals become unstable. The resulting dehydration reactions are strongly temperature-dependent, and due to the solid solutions of the minerals involved, this dehydration is a continuously evolving process driven by the steady, slow heat flow into the plate, Fig. 1 right. Evidence from the global volatile budget indicates [vKHSA11] that there must be a fluid escape mechanism that can keep pace with the slab descent velocity (cm/year) to avoid the fluid being lost to the earth interior. This dynamic fluid escape mechanism leads fluid flow to organize itself into large-scale and high-flux transport systems through which fluids can escape from the subducting plate, cf. e.g., [vKHSA11, PJP$^+$17]. In fact, it has been shown in various field-based studies that intra-slab fluid flow and fluid escape from the slab are channelized and reactive, cf. e.g., [CHJ$^+$19, JGP$^+$12, APDH$^+$14, HJBS12, TJB$^+$18, PNTG$^+$10].

Dehydration reactions often lead to a densification of the solid phases of the plate and thus to the formation of a fluid-filled porosity. The initial porosity forms at the sub-mm scale and is heterogeneously distributed across the rock as defined by the local bulk composition [PJP$^+$17]. As dehydration progresses, these initial vein-like porosity structures merge and form a vein network that allows fluid flow in the rock [JKGGS08, TJB$^+$18, PJP$^+$17, BJK$^+$18, CPNT19]. Hereby, reactive fluid flow is able to trigger further rock dehydration and to transform an initially fine and small-scale high-porosity structure into wider and larger vein systems that may also develop reaction halos [HVJ22] by chemical interaction with the wall rock, cf. also [TJB$^+$18, JGP$^+$12]. The works [PJP$^+$17, BJV$^+$20, HVJ22] develop thermodynamically consistent porous-media models which explain the generation of porosity and veining due to dehydration reactions. They provide a first step towards a mechanistic understanding on how dehydration leads from the first stage of chemistry-controlled local dehydration to the development of intra-slab flow structures that are highly channelized. These channels may show only limited interaction with the wall rock, cf. e.g., [BA02, SPR11, HJBS12], but they may also have well-developed reaction halos, cf. e.g., [TJB$^+$18, JGP$^+$12, HVJ22].

In this work we discuss the porous-media models developed in [PJP$^+$17, BJV$^+$20, HVJ22] in more detail from a mathematical point of view. In particular, the porous-media model deduced in [PJP$^+$17] takes the following form

$$\partial_t\big(\hat{\varrho}_{\mathrm{s}}(1-X_{\mathrm{h}})(1-\phi)\big) = 0\,, \tag{1.1a}$$

$$\partial_t\big(\hat{\varrho}_{\mathrm{s}}(1-\phi) + \hat{\varrho}_{\mathrm{f}}\phi\big) = \nabla\cdot\Big(\hat{\varrho}_{\mathrm{f}}K(\phi)\nabla\pi\Big)\,. \tag{1.1b}$$

DOI 10.20347/WIAS.PREPRINT.2999 Berlin 2023

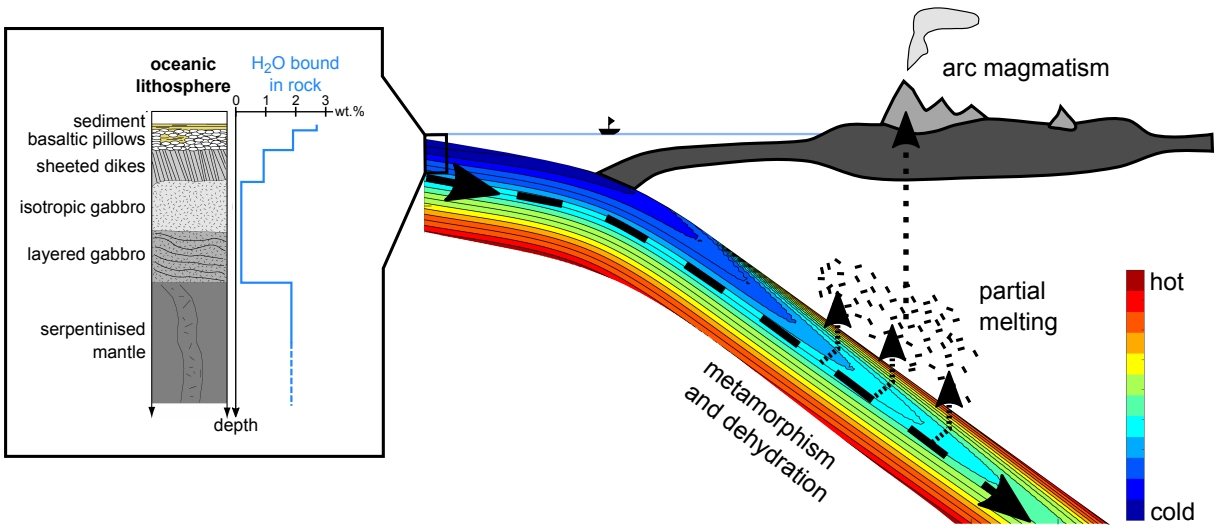

Figure 1: Schematic view of a subducting slab that heats up from top and below and therefore dehydrates on its way into the hot earth mantle. Colors within the slab indicate temperature. The left box shows a typical profile through the uppermost part of the slab as it enters the subduction zone. Different lithologies contain various amounts of H_2O that is bound in hydrous minerals. On its decent into the mantle the slab is heated up by heat conduction from the surrounding mantle. Increasing temperatures lead to dehydration, i.e. the release of the rock-bound H_2O in a free fluid phase (small dashed arrows). These fluids cause partial melting of the mantle which gives rise to arc magmatism at the surface. Dimensions are not to scale. Rock-bound H_2O contents are taken from [RMHC04].

Here, ϕ denotes the porosity, π the fluid pressure, and X_h the H_2O-content of the solid phase. Moreover, with index $i \in \{\mathrm{f}, \mathrm{s}\}$ for fluid and solid $\hat{\varrho}_\mathrm{i}$ denotes the "pure" mass density of the respective phase and the expression $K(\phi)$ is a Kozeny–Carman-type permeability of the form $K(\phi) = \frac{\kappa}{\mu}\phi^3$ with positive constants $\kappa, \mu > 0$. In this way, (1.1a) expresses the conservation of mass for the immobile solid and (1.1b) provides the conservation of total mass. Given suitable initial data, one observes that (1.1a) may be explicitly solved for the porosity

$$\phi = 1 - \frac{\hat{\varrho}_\mathrm{s}^0(1-X_\mathrm{h}^0)(1-\phi^0)}{\hat{\varrho}_\mathrm{s}(1-X_\mathrm{h})},$$

where quantities with superscript 0 denote given initial data. Additionally, the models studied in [BJV$^+$20, HVJ22] also take into account the influence of further chemical species transported with the fluid on the dehydration process. This chemical species is CO_2 in [BJV$^+$20] and SiO_2 in [HVJ22]. It is assumed to undergo a diffusion process in the fluid phase, so that the model in [HVJ22] reads:

$$\partial_t\big(\hat{\varrho}_\mathrm{s}(1-\phi) + \hat{\varrho}_\mathrm{f}\phi\big) = \nabla\cdot\Big(\hat{\varrho}_\mathrm{f}K(\phi)\nabla\pi\Big), \tag{1.2a}$$

$$\partial_t\big(\hat{\varrho}_\mathrm{s}c_\mathrm{s}(1-\phi) + \hat{\varrho}_\mathrm{f}c_\mathrm{f}\phi\big) = \nabla\cdot\Big(\hat{\varrho}_\mathrm{f}c_\mathrm{f}K(\phi)\nabla\pi + \hat{\varrho}_\mathrm{f}c_\mathrm{f}\phi D_c\nabla c_\mathrm{f}\Big), \tag{1.2b}$$

$$\phi = 1 - \frac{\hat{\varrho}_\mathrm{s}^0(1-c_\mathrm{s}^0-X_\mathrm{h}^0)(1-\phi^0)}{\hat{\varrho}_\mathrm{s}(1-c_\mathrm{s}-X_\mathrm{h})}, \tag{1.2c}$$

where ϕ, π, X_h, $\hat{\varrho}_\mathrm{f}$, $\hat{\varrho}_\mathrm{s}$, and $K(\phi)$ have the same meaning as in (1.1). In addition, with index $i \in \{\mathrm{f}, \mathrm{s}\}$ for fluid and solid c_i is the SiO_2-content of the respective phase and D_c in (1.2b) is a diffusion coefficient. Again, quantities with superscript 0 denote given initial data. In [PJP$^+$17], resp. [HVJ22], systems (1.1) and (1.2) are numerically solved for the unknowns ϕ, π, and c_s by a finite difference method, whereas the the

remaining quantities $c_{\mathrm{f}} = \tilde{c}_{\mathrm{f}}(\pi, c_{\mathrm{s}}, \theta)$, $X_{\mathrm{h}} = \tilde{X}_{\mathrm{h}}(\pi, c_{\mathrm{s}}, \theta)$, $\hat{\varrho}_i = \tilde{\hat{\varrho}}_i(\pi, c_{\mathrm{s}}, \theta)$, $i \in \{\mathrm{s}, \mathrm{f}\}$, implicitly depend on the unknowns and on the (given) temperature θ. Their values are obtained from equilibrium thermodynamical closing relations.

In this present work we further discuss models (1.1) and (1.2) from a mathematical point of view. First, based on our findings in [ZPT21], we investigate the thermodynamical structure of models (1.1) and (1.2) in the framework GENERIC (the acronym for General Equations of Non-Equilibrium Reversible Irreversible Coupling). For this, we briefly review the modeling concept of GENERIC in Section 2 and use it to develop a model for reactive two-phase Darcy flows, cf. Sec. 2.3. Many porous-media models in literature also consider chemical reactions in a thermodynamically consistent way, cf. e.g. [OSC15, Ehl09]. Yet, many treat reactions only within a phase or the exchange of mass between the different phases is incorporated by rather heuristic exchange terms [Cou04, ADDN04, Kra14]. The reactive two-phase Darcy-flow model, that we obtain with the aid of the GENERIC framework, allows for the exchange of mass between the different phases by chemical reactions, where the corresponding reaction terms are directly inferred from the thermodynamical functionals and dissipative operators related to the chemical reactions. In this way the exchange process is incorporated in a thermodynamically consistent way and the structure of the process including the reaction kinetics is highlighted very well.

As mentioned above, in the works [PJP$^+$17, BJV$^+$20, HVJ22] the determination of the quantities c_{f}, X_{h} $\hat{\varrho}_{\mathrm{s}}$, and $\hat{\varrho}_{\mathrm{f}}$ stems from equilibrium thermodynamical closing relations deduced by Gibbs minimization. This approach rests on the assumption that chemical reactions take place on much faster time scales than flow and transport so that they can be assumed to be in local equilibrium. In Section 3 we therefore discuss the local equilibrium of fast dissipative processes in the GENERIC framework and deduce equations for the effective system. For this, we follow the ideas of [MPS21]. We apply this approach to the equilibration of temperature in the two-phase system and to the equilibration of chemical reactions. These considerations put us in the position to show in Section 4 that the models (1.1) and (1.2) originate from the reactive two-phase Darcy flow model deduced in Sec. 2.3 by equilibration of the fast reactions. Finally, Section 5 provides first analytical results on the existence of weak solutions for the models. Here we take into account the discretization scheme used in [HVJ22] for the numerical simulations and we critically discuss the mathematical assumptions with respect to the evidence of the thermodynamical properties given by the chemical composition of the rock samples considered in [PJP$^+$17, HVJ22].

2 GENERIC structure of reactive two-phase systems

Short introduction to the GENERIC framework The thermodynamical modeling framework of GENERIC (General Equations of Non-Equilibrium Reversible Irreversible Coupling) was introduced by Öttinger and Grmela in [GÖ97, ÖG97]. It characterizes the evolution of a thermodynamical system in terms of a state space $\mathcal{Q}$ with dual $\mathcal{Q}^*$, thermodynamical potentials such as energy $\mathcal{E}$ and entropy $\mathcal{S}$, and geometric structures $\mathbb{J}$ and $\mathbb{K}$, which encode the reversible (Hamiltonian) or irreversible (Onsager) nature of the process. Characteristically for this, the Poisson structure $\mathbb{J}(\boldsymbol{q}) : \mathcal{Q}^* \to \mathcal{Q}$ is antisymmetric $\mathbb{J}^* = -\mathbb{J}$ and satisfies Jacobi's identity, whereas the Onsager operator $\mathbb{K}(\boldsymbol{q}) : \mathcal{Q}^* \to \mathcal{Q}$ is positively semidefinite $\langle \xi, \mathbb{K}(\boldsymbol{q})\xi \rangle \geq 0$ for all $\xi \in \mathcal{Q}^*$ and symmetric $\mathbb{K}^* = \mathbb{K}$. The triple $(\mathcal{Q}, \mathcal{E}, \mathbb{J})$ forms a Hamiltonian system for reversible dynamics and the triple $(\mathcal{Q}, \mathcal{S}, \mathbb{K})$ forms an Onsager, resp. gradient system for dissipative dynamics. A GENERIC system $(\mathcal{Q}, \mathcal{E}, \mathcal{S}, \mathbb{J}, \mathbb{K})$ couples the two via the non-interaction conditions (NIC)

$$\mathbb{J}(\boldsymbol{q})\mathrm{D}\mathcal{S}(\boldsymbol{q}) = 0 = \mathbb{K}(\boldsymbol{q})\mathrm{D}\mathcal{E}(\boldsymbol{q})\,, \tag{2.1}$$

Symbol(s)	Unit	Definition	Reference
Ω		Spatial domain in $\mathbb{R}^d$	(2.4)
$\boldsymbol{v}_i$	m s^{-1}	Velocity of solid-s and fluid-f	(2.5)
$\boldsymbol{P}_i$		Momentum density of solid-s and fluid-f	(2.9)
$\boldsymbol{C}_i$		Concentration density vector of solid-s and fluid-f	(2.9),(2.10), Ex. 2.1
U_i	J m^{-3}	Internal energy density of solid-s and fluid-f	(2.9)
S_i	J K^{-1} m^{-3}	Entropy density of solid-s and fluid-f	(2.1),(2.11),(2.22)
E_i	J m^{-3}	Total energy density of solid-s and fluid-f	(2.1),(2.11)
$\boldsymbol{M}_i$	kg mol^{-1}	Vector of molar masses of solid-s and fluid-f	(2.10),Ex. 2.1
ϱ_i	kg m^{-3}	Mass density of solid-s and fluid-f	(2.10)
π_i	Pa	Pressure of solid-s and fluid-f	(2.12)
θ_i	K	Temperature of solid-s and fluid-f	(2.12)
μ_i	J mol^{-1}	Chemical potential of solid-s and fluid-f	(2.12)
ϕ	vol. fr.	Porosity	(1.1), (1.2), Sec. 4.2
$\hat{\varrho}_\mathrm{i}$	kg m^{-3}	"pure" mass density of solid-s and fluid-f	(1.1), (1.2), (4.6)
$c_\mathrm{f}, c_\mathrm{s}$	wt. fr.	SiO_2 content of solid-s and fluid-f	Sec. 4.3
X_h	wt. fr.	H_2O in solid	(1.2), Sec. 4.2
$\boldsymbol{q}$		State vector	Sec. 2, (2.9)
$\dot{\boldsymbol{q}} = \partial_t \boldsymbol{q}$		Partial time derivative of $\boldsymbol{q}$	(1.1),(1.2),(2.3)
$\mathcal{Q}, \mathcal{Q}^*$		State space and its dual	Sec. 2
$\boldsymbol{\eta}, \boldsymbol{\xi}$		Element of $\mathcal{Q}^*$	(2.19a)
$\mathcal{E}$	J	Total energy functional	Sec. 2, (2.11)
$\mathcal{S}$	J K^{-1}	Total entropy functional	Sec. 2, (2.11), (2.22)
$\mathbb{J}$		Poisson operator	Sec. 2, (2.14)
$\mathbb{K}$		Onsager operator	Sec. 2, (2.15),(2.24)
$\mathrm{D}\mathcal{A}$		Functional derivative	Sec. 2, (2.13)
T		Transformation between state spaces	
$\mathbb{L}, \mathbb{L}^*$		Fréchet derivative of T, $\mathbb{L} := \mathrm{DT}$ and its adjoint $\mathbb{L}^*$	

Table 1: List of most recurring symbols with references to definitions, sections and relevant examples.

and the mass conservation condition

$$\mathbb{J}(\boldsymbol{q})\mathrm{D}\mathcal{M}(\boldsymbol{q}) = 0 = \mathbb{K}(\boldsymbol{q})\mathrm{D}\mathcal{M}(\boldsymbol{q}) \tag{2.2}$$

for the total mass $\mathcal{M}$ of the system. We call conditions (2.1) and (2.2) degeneracy conditions. Above, D denotes the Fréchet derivative of the driving functional with respect to $\boldsymbol{q}$. The properties of $\mathbb{J}$ and $\mathbb{K}$ together with the NIC (2.1) ensure the compatibility of the system with the laws of thermodynamics and (2.2) ensures the conservation of the total mass of the system. The evolution of a state vector $\boldsymbol{q} : [0, \mathsf{T}] \to \mathcal{Q}$ describing the mechanical and thermodynamical properties of the system is then given by

$$\partial_t \boldsymbol{q} = \mathbb{J}(\boldsymbol{q})\mathrm{D}\mathcal{E}(\boldsymbol{q}) + \mathbb{K}(\boldsymbol{q})\mathrm{D}\mathcal{S}(\boldsymbol{q})\,. \tag{2.3}$$

For more details on the GENERIC framework we refer to [GÖ97, ÖG97] and with regard to transformation properties of GENERIC systems also to [ZPT21].

In [ZPT21] we discussed the GENERIC framework for reactive fluid flows. In this section we extend these results to multiphase systems. For this, we will introduce a two-phase Darcy model in Sec. 2.1 and study a multiphase system with diffusion and chemical reactions between the two phases in Sec. 2.2. Subsequently, we will combine these results in Sec. 2.3 to obtain the GENERIC structure of reactive two-phase Darcy flows.

Kinematics of two-phase flows We follow here the approach to the theory of porous media as outlined e.g. in [Ehl09] and describe the two-phase system, consisting of a fluid (f) and a solid (s) phase, in the Eulerian frame, where $\Omega(t) \subset \mathbb{R}^d$ denotes the domain in Eulerian coordinates at time $t \in [0, \mathsf{T}]$. To each phase $i \in \{\mathrm{f}, \mathrm{s}\}$ there is an associated reference domain $\bar{\Omega}_i \subset \mathbb{R}^d$ and a sufficiently smooth flow map $\bar{\boldsymbol{\chi}}_i : [0, \mathsf{T}] \times \bar{\Omega}_i \to \mathbb{R}^d$, $(t, \bar{\boldsymbol{x}}) \in [0, \mathsf{T}] \times \bar{\Omega}_i \mapsto \boldsymbol{x} = \bar{\boldsymbol{\chi}}_i(t, \bar{\boldsymbol{x}}) \in \Omega(t)$, so that

$$\Omega(t) := \{\boldsymbol{x} \in \mathbb{R}^d,\, \boldsymbol{x} = \bar{\boldsymbol{\chi}}_i(t, \bar{\boldsymbol{x}}_i) \text{ for some } \bar{\boldsymbol{x}}_i \in \bar{\Omega}_i\} \;\text{ for } i \in \{\mathrm{s}, \mathrm{f}\}\,. \tag{2.4}$$

When there is no chance for misunderstanding we omit indicating the time dependence of the current configuration, i.e., we write Ω for $\Omega(t)$. The motion of phase i is characterized by the following ODE Cauchy problem

$$\partial_t \bar{\boldsymbol{\chi}}_i(t, \bar{x}) = \boldsymbol{v}_i(t, \bar{\boldsymbol{\chi}}_i(t, \bar{x})) \qquad \text{for all } \bar{x} \in \bar{\Omega}_i,\, t \in [0, \mathsf{T}]\,, \tag{2.5a}$$

$$\bar{\boldsymbol{\chi}}_i(0, \bar{x}) = \bar{x} \qquad \text{for all } \bar{x} \in \bar{\Omega}_i\,, \tag{2.5b}$$

where $\boldsymbol{v}_i : [0, \mathsf{T}] \times \Omega(t) \to \mathbb{R}^d$ denotes the Eulerian velocity field of phase i and we ask that

$$\boldsymbol{v}_{\mathrm{s}}(t, \cdot) = \boldsymbol{v}_{\mathrm{f}}(t, \cdot) \;\text{ on }\; \partial\Omega(t)\,. \tag{2.6}$$

In order to ensure that the flow map is orientation-preserving we claim that its Jacobi determinant is positive, i.e.,

$$\bar{V}_i := \det \bar{\nabla} \bar{\boldsymbol{\chi}}_i > 0\,, \tag{2.7}$$

and we denote the Jacobi matrix by

$$F_i := \bar{\nabla} \bar{\boldsymbol{\chi}}_i\,, \quad \text{where } (F_i)_{kl} = (\bar{\nabla} \bar{\boldsymbol{\chi}}_i)_{kl} = (\partial_{\bar{x}_l} (\bar{\boldsymbol{\chi}}_i)_k) \tag{2.8}$$

where $\bar{\boldsymbol{x}} = (\bar{x}_1, \dots, \bar{x}_d)^\top$ are the coordinates of the Lagrangian domain $\bar{\Omega}_i$ of phase i.

2.1 Two-phase Darcy flow

We now deduce the GENERIC structure for a two-phase Darcy model without reactions but with an interphase friction term. For this we extend our findings from [ZPT21, Sec. 6] to the two-phase setting. To keep the presentation concise, we directly start the considerations in Eulerian coordinates. As described above, the state $\boldsymbol{q} \in \mathcal{Q}$ of the multiphase flow is defined by a vector of fluid (f) and solid (s) quantities

$$\boldsymbol{q} = \begin{pmatrix} \boldsymbol{q}_{\mathrm{s}} \\ \boldsymbol{q}_{\mathrm{f}} \end{pmatrix} = \begin{pmatrix} \boldsymbol{P}_{\mathrm{s}} : \Omega \to \mathbb{R}^d \\ \boldsymbol{C}_{\mathrm{s}} : \Omega \to \mathbb{R}^{N_{\mathrm{s}}} \\ U_{\mathrm{s}} : \Omega \to \mathbb{R} \\ \boldsymbol{P}_{\mathrm{f}} : \Omega \to \mathbb{R}^d \\ \boldsymbol{C}_{\mathrm{f}} : \Omega \to \mathbb{R}^{N_{\mathrm{f}}} \\ U_{\mathrm{f}} : \Omega \to \mathbb{R} \end{pmatrix}. \tag{2.9}$$

In each phase $i \in \{\mathrm{s}, \mathrm{f}\}$ there are N_i components with a vector of concentrations $\boldsymbol{C}_i = (C_{i,k})_{k=1}^{N_i} \in \mathbb{R}^{N_i}$ and a corresponding vector of molar masses $\boldsymbol{M}_i = (M_{i,k})_{k=1}^{N_i} \in \mathbb{R}^{N_i}$, such that each phase has the mass density ϱ_i and the total mass density is ϱ_{tot} defined by

$$\varrho_i = \sum_{k=1}^{N_i} M_{i,k} C_{i,k} = \boldsymbol{M}_i \cdot \boldsymbol{C}_i \quad \text{and} \quad \varrho_{\mathrm{tot}} = \varrho_{\mathrm{s}} + \varrho_{\mathrm{f}}. \tag{2.10}$$

Additionally, each phase has a separate momentum $\boldsymbol{P}_i$ and internal energy U_i. At this point we observe that the quantities here defined account already for the volume fraction of the respective phase. Definitions of "pure" and "partial" quantities and their relation to volume fractions are treated in Sec. 4.2.

Above notation allows us to define the functionals for total energy $\mathcal{E}$ and entropy $\mathcal{S}$ as

$$\mathcal{E}(\boldsymbol{q}) := \int_\Omega E_{\mathrm{s}}(\boldsymbol{q}_{\mathrm{s}}) + E_{\mathrm{f}}(\boldsymbol{q}_{\mathrm{f}}) \,\mathrm{d}\boldsymbol{x} \quad \text{with} \quad E_i(\boldsymbol{q}_i) = \frac{|\boldsymbol{P}_i|^2}{2\varrho_i} + U_i \,, \tag{2.11a}$$

$$\mathcal{S}(\boldsymbol{q}) := \int_\Omega S_{\mathrm{s}}(\boldsymbol{C}_{\mathrm{s}}, U_{\mathrm{s}}) + S_{\mathrm{f}}(\boldsymbol{C}_{\mathrm{f}}, U_{\mathrm{f}}) \,\mathrm{d}\boldsymbol{x} \,, \tag{2.11b}$$

where the total energy and entropy densities are $E = E_{\mathrm{s}} + E_{\mathrm{f}}$ and $S = S_{\mathrm{s}} + S_{\mathrm{f}}$. The entropies satisfy the Gibbs relations

$$\frac{\pi_i}{\theta_i} := S_i - \boldsymbol{C}_i \partial_{\boldsymbol{C}_i} S_i - U_i \partial_{U_i} S_i, \qquad \frac{1}{\theta_i} := \partial_{U_i} S_i, \qquad \frac{\mu_i}{\theta_i} := \partial_{\boldsymbol{C}_i} S_i \tag{2.12}$$

separately for each phase $i \in \{\mathrm{s}, \mathrm{f}\}$ with pressure π_i, temperature θ_i, and chemical potential μ_i. This gives the driving forces for the GENERIC evolution as

$$\mathrm{D}\mathcal{E}(\boldsymbol{q}) = \boldsymbol{\eta} = \begin{pmatrix} \boldsymbol{P}_{\mathrm{s}}/\varrho_{\mathrm{s}} \\ 0 \\ 1 \\ \boldsymbol{P}_{\mathrm{f}}/\varrho_{\mathrm{f}} \\ 0 \\ 1 \end{pmatrix}, \qquad \mathrm{D}\mathcal{S}(\boldsymbol{q}) = \boldsymbol{\xi} = \begin{pmatrix} 0 \\ \mu_{\mathrm{s}}/\theta_{\mathrm{s}} \\ 1/\theta_{\mathrm{s}} \\ 0 \\ \mu_{\mathrm{f}}/\theta_{\mathrm{f}} \\ 1/\theta_{\mathrm{f}} \end{pmatrix}, \tag{2.13}$$

where we will denote with the subscript $\mathrm{D}_a\mathcal{A}, \xi_a$ and η_a the a-component of the vectors $\mathrm{D}\mathcal{A}, \boldsymbol{\xi}, \boldsymbol{\eta}$. The reversible dynamics of the system follows the evolution given by the Poisson structure

$$\mathbb{J}(\boldsymbol{q}) = \begin{pmatrix} \mathbb{J}_{\boldsymbol{P}_{\mathrm{s}}\boldsymbol{P}_{\mathrm{s}}} & \mathbb{J}_{\boldsymbol{P}_{\mathrm{s}}\boldsymbol{C}_{\mathrm{s}}} & \mathbb{J}_{\boldsymbol{P}_{\mathrm{s}}U_{\mathrm{s}}} & 0 & 0 & 0 \\ \mathbb{J}_{\boldsymbol{C}_{\mathrm{s}}\boldsymbol{P}_{\mathrm{s}}} & 0 & 0 & 0 & 0 & 0 \\ \mathbb{J}_{U_{\mathrm{s}}\boldsymbol{P}_{\mathrm{s}}} & 0 & 0 & 0 & 0 & 0 \\ 0 & 0 & 0 & \mathbb{J}_{\boldsymbol{P}_{\mathrm{f}}\boldsymbol{P}_{\mathrm{f}}} & \mathbb{J}_{\boldsymbol{P}_{\mathrm{f}}\boldsymbol{C}_{\mathrm{f}}} & \mathbb{J}_{\boldsymbol{P}_{\mathrm{f}}U_{\mathrm{f}}} \\ 0 & 0 & 0 & \mathbb{J}_{\boldsymbol{C}_{\mathrm{f}}\boldsymbol{P}_{\mathrm{f}}} & 0 & 0 \\ 0 & 0 & 0 & \mathbb{J}_{U_{\mathrm{f}}\boldsymbol{P}_{\mathrm{f}}} & 0 & 0 \end{pmatrix} \quad \text{with} \quad \begin{aligned} \mathbb{J}_{\boldsymbol{P}_i\boldsymbol{P}_i}\square &:= -(\nabla\square)^\top \boldsymbol{P}_i - \nabla\cdot(\boldsymbol{P}_i \otimes \square)\,, \\ \mathbb{J}_{\boldsymbol{P}_i\boldsymbol{C}_i}\square &:= -(\nabla\square)^\top \boldsymbol{C}_i\,, \\ \mathbb{J}_{\boldsymbol{C}_i\boldsymbol{P}_i}\square &:= -\nabla\cdot(\boldsymbol{C}_i \otimes \square)\,, \\ \mathbb{J}_{\boldsymbol{P}_iU_i}\square &:= -U_i\nabla\square + \nabla(\square\pi_i)\,, \\ \mathbb{J}_{U_i\boldsymbol{P}_i}\square &:= -\nabla\cdot(U_i\square) + \pi_i\nabla\cdot\square\,. \end{aligned} \tag{2.14}$$

The irreversible processes are encoded in an Onsager operator

$$\mathbb{K}(\boldsymbol{q}) = \begin{pmatrix} \mathbb{K}_{\mathrm{ss}}(\boldsymbol{q}) & \mathbb{K}_{\mathrm{sf}}(\boldsymbol{q}) \\ \mathbb{K}_{\mathrm{fs}}(\boldsymbol{q}) & \mathbb{K}_{\mathrm{ff}}(\boldsymbol{q}) \end{pmatrix} = \begin{pmatrix} \mathbb{K}^{\mathrm{s}}_{\mathrm{visc}} + \mathbb{K}^{\mathrm{s}}_{\mathrm{ht}} & 0 \\ 0 & \mathbb{K}^{\mathrm{f}}_{\mathrm{visc}} + \mathbb{K}^{\mathrm{f}}_{\mathrm{ht}} \end{pmatrix} + \begin{pmatrix} \mathbb{K}^{\mathrm{ss}}_{\mathrm{he}} + \mathbb{K}^{\mathrm{ss}}_{\mathrm{fric}} & \mathbb{K}^{\mathrm{sf}}_{\mathrm{he}} + \mathbb{K}^{\mathrm{sf}}_{\mathrm{fric}} \\ \mathbb{K}^{\mathrm{fs}}_{\mathrm{he}} + \mathbb{K}^{\mathrm{fs}}_{\mathrm{fric}} & \mathbb{K}^{\mathrm{ff}}_{\mathrm{he}} + \mathbb{K}^{\mathrm{ff}}_{\mathrm{fric}} \end{pmatrix}, \tag{2.15}$$

where each of the blocks $\mathbb{K}_{ji}$ for $i,j \in \{\mathrm{s},\mathrm{f}\}$ is a 3×3 block acting on the derivatives of $\mathcal{S}$ with respect to $\boldsymbol{q}_i = (\boldsymbol{P}_i, \boldsymbol{C}_i, U_i)^\top$. Single-phase effects are solely encoded in the diagonal operators $\mathbb{K}_{\mathrm{ss}}, \mathbb{K}_{\mathrm{ff}}$ and interaction terms are encoded in all the components of $\mathbb{K}$. We consider irreversible processes due to single-phase Stokesian viscous dissipation $\mathbb{K}^i_{\mathrm{visc}}$ and heat transport $\mathbb{K}^i_{\mathrm{ht}}$. Phase interaction is due to interfacial friction $\mathbb{K}^{ij}_{\mathrm{fric}}$ and due to heat exchange $\mathbb{K}^{ij}_{\mathrm{he}}$. First we consider the single-phase effect of viscous dissipation

$$\mathbb{K}^i_{\mathrm{visc}} = \begin{pmatrix} \mathbb{K}^{\mathrm{visc},i}_{\boldsymbol{PP}} & 0 & \mathbb{K}^{\mathrm{visc},i}_{\boldsymbol{P}U} \\ 0 & 0 & 0 \\ \mathbb{K}^{\mathrm{visc},i}_{U\boldsymbol{P}} & 0 & \mathbb{K}^{\mathrm{visc},i}_{UU} \end{pmatrix} \quad \text{with} \quad \begin{aligned} \mathbb{K}^{\mathrm{visc},i}_{\boldsymbol{PP}}\Box &:= -\nabla\cdot\big(2\theta_i\lambda_i\nabla_{\mathrm{s}}\Box + \theta_i\zeta_i\mathrm{tr}(\nabla_{\mathrm{s}}\Box)\mathbb{I}_d\big)\,, \\ \mathbb{K}^{\mathrm{visc},i}_{UU}\Box &:= \big(2\theta_i\lambda_i|\nabla_{\mathrm{s}}\boldsymbol{v}_i|^2 + \theta_i\zeta_i\,\mathrm{tr}(\nabla_{\mathrm{s}}\boldsymbol{v}_i)^2\big)\Box\,, \\ \mathbb{K}^{\mathrm{visc},i}_{U\boldsymbol{P}}\Box &:= -\big(2\theta_i\lambda_i\nabla_{\mathrm{s}}\Box + \theta_i\zeta_i\mathrm{tr}(\nabla_{\mathrm{s}}\Box)\mathbb{I}_d\big){:}\nabla\boldsymbol{v}_i\,, \\ \mathbb{K}^{\mathrm{visc},i}_{\boldsymbol{P}U}\Box &:= \nabla\cdot\big((2\theta_i\lambda_i\nabla_{\mathrm{s}}\boldsymbol{v}_i + \theta_i\zeta_i\mathrm{tr}(\nabla_{\mathrm{s}}\boldsymbol{v}_i)\mathbb{I}_d)\Box\big)\,, \end{aligned} \tag{2.16}$$

where λ_i, ζ_i are the viscous parameter of the solid and fluid Stokes dissipation and $\boldsymbol{v}_i = \boldsymbol{P}_i/\varrho_i$ the single-phase velocity. Furthermore we have the symmetric gradient $\nabla_{\mathrm{s}}\Box = \frac{1}{2}(\nabla\Box + \nabla\Box^\top)$. The heat conduction is given by the operator

$$\mathbb{K}^i_{\mathrm{ht}} = \begin{pmatrix} 0 & 0 & 0 \\ 0 & 0 & 0 \\ 0 & 0 & \mathbb{K}^{\mathrm{ht},i}_{UU} \end{pmatrix} \quad \text{with} \quad \mathbb{K}^{\mathrm{ht},i}_{UU}\Box := -\nabla\cdot(\theta_i^2 k_i\nabla\Box)\,, \tag{2.17}$$

where k_i is the heat conduction of each phase. The heat exchange is of the 6×6 block form

$$\begin{pmatrix} \mathbb{K}^{\mathrm{ss}}_{\mathrm{he}} & \mathbb{K}^{\mathrm{sf}}_{\mathrm{he}} \\ \mathbb{K}^{\mathrm{fs}}_{\mathrm{he}} & \mathbb{K}^{\mathrm{ff}}_{\mathrm{he}} \end{pmatrix} = k_{\mathrm{he}}(\boldsymbol{q}) \begin{pmatrix} 0 & 0 & 0 & 0 & 0 & 0 \\ 0 & 0 & 0 & 0 & 0 & 0 \\ 0 & 0 & +1 & 0 & 0 & -1 \\ 0 & 0 & 0 & 0 & 0 & 0 \\ 0 & 0 & 0 & 0 & 0 & 0 \\ 0 & 0 & -1 & 0 & 0 & +1 \end{pmatrix} \tag{2.18}$$

for some some given heat exchange coefficient function $k_{\mathrm{he}}(\boldsymbol{q}) \geq 0$. The isotropic Darcy interaction between the two phases is generated by the dual dissipation potential

$$\Psi^*_{\mathrm{fric}}(\boldsymbol{q},\boldsymbol{\xi}) = \int_\Omega \frac{K_{\mathrm{D}}}{2}\frac{\theta_{\mathrm{s}}\theta_{\mathrm{f}}}{\theta_{\mathrm{s}}+\theta_{\mathrm{f}}}|\boldsymbol{w}|^2\,\mathrm{d}\boldsymbol{x}\,, \tag{2.19a}$$

where $\boldsymbol{w} = \xi_{\boldsymbol{P}_{\mathrm{s}}} - \xi_{\boldsymbol{P}_{\mathrm{f}}} - (\alpha\xi_{U_{\mathrm{s}}} + (1-\alpha)\xi_{U_{\mathrm{f}}})\boldsymbol{\gamma}$. Here $\boldsymbol{\gamma} = (\boldsymbol{v}_{\mathrm{s}} - \boldsymbol{v}_{\mathrm{f}})$ and $\alpha(\boldsymbol{q}) \in (0,1)$ is arbitrary and controls how much of the generated entropy is converted into heat of the solid and fluid phase, respectively. The Onsager operator corresponding to this dual dissipation is

$$\mathbb{K}_{\mathrm{fric}} = K_{\mathrm{D}}(\boldsymbol{q})\frac{\theta_{\mathrm{s}}\theta_{\mathrm{f}}}{\theta_{\mathrm{s}}+\theta_{\mathrm{f}}} \begin{pmatrix} +1 & 0 & -\boldsymbol{\gamma}\alpha & -1 & 0 & -\boldsymbol{\gamma}(1-\alpha) \\ 0 & 0 & 0 & 0 & 0 & 0 \\ -\boldsymbol{\gamma}\alpha & 0 & \boldsymbol{\gamma}^2\alpha^2 & \boldsymbol{\gamma}\alpha & 0 & |\boldsymbol{\gamma}|^2\alpha(1-\alpha) \\ -1 & 0 & \boldsymbol{\gamma}\alpha & +1 & 0 & \boldsymbol{\gamma}(1-\alpha) \\ 0 & 0 & 0 & 0 & 0 & 0 \\ -\boldsymbol{\gamma}(1-\alpha) & 0 & |\boldsymbol{\gamma}|^2\alpha(1-\alpha) & \boldsymbol{\gamma}(1-\alpha) & 0 & |\boldsymbol{\gamma}|^2(1-\alpha)^2 \end{pmatrix}. \tag{2.19b}$$

Based on these definitions, the GENERIC evolution of the compressible two-phase flow reads

$$\dot{\boldsymbol{P}}_{\mathrm{s}} + \nabla \cdot (\boldsymbol{P}_{\mathrm{s}} \otimes \boldsymbol{v}_{\mathrm{s}}) = -\nabla \pi_{\mathrm{s}} - K_{\mathrm{D}} \boldsymbol{\gamma} + \nabla \cdot \boldsymbol{\sigma}_{\mathrm{s}}\,, \tag{2.20a}$$

$$\dot{\boldsymbol{P}}_{\mathrm{f}} + \nabla \cdot (\boldsymbol{P}_{\mathrm{f}} \otimes \boldsymbol{v}_{\mathrm{f}}) = -\nabla \pi_{\mathrm{f}} + K_{\mathrm{D}} \boldsymbol{\gamma} + \nabla \cdot \boldsymbol{\sigma}_{\mathrm{f}}\,, \tag{2.20b}$$

$$\dot{\boldsymbol{C}}_{\mathrm{s}} + \nabla \cdot (\boldsymbol{C}_{\mathrm{s}} \otimes \boldsymbol{v}_{\mathrm{s}}) = 0\,, \tag{2.20c}$$

$$\dot{\boldsymbol{C}}_{\mathrm{f}} + \nabla \cdot (\boldsymbol{C}_{\mathrm{f}} \otimes \boldsymbol{v}_{\mathrm{f}}) = 0\,, \tag{2.20d}$$

$$\dot{U}_{\mathrm{s}} + \nabla \cdot (U_{\mathrm{s}} \boldsymbol{v}_{\mathrm{s}}) = -\pi_{\mathrm{s}} \nabla \cdot \boldsymbol{v}_{\mathrm{s}} + \alpha K_{\mathrm{D}} |\boldsymbol{\gamma}|^2 + k_{\mathrm{he}} (\theta_{\mathrm{s}}^{-1} - \theta_{\mathrm{f}}^{-1}) + \nabla \cdot (k_{\mathrm{s}} \nabla \theta_{\mathrm{s}})\,, \tag{2.20e}$$

$$\dot{U}_{\mathrm{f}} + \nabla \cdot (U_{\mathrm{f}} \boldsymbol{v}_{\mathrm{f}}) = -\pi_{\mathrm{f}} \nabla \cdot \boldsymbol{v}_{\mathrm{f}} + (1-\alpha) K_{\mathrm{D}} |\boldsymbol{\gamma}|^2 - k_{\mathrm{he}} (\theta_{\mathrm{s}}^{-1} - \theta_{\mathrm{f}}^{-1}) + \nabla \cdot (k_{\mathrm{f}} \nabla \theta_{\mathrm{f}})\,, \tag{2.20f}$$

with the Cauchy stress tensor $\boldsymbol{\sigma}_i = 2\lambda_i (\nabla_{\mathrm{s}} \boldsymbol{v}_i) + \zeta_i (\nabla \cdot \boldsymbol{v}_i) \mathbb{I}_d$ for each phase. Using the fundamental Gibbs relation (2.12) one can verify that $\mathbb{J}(\boldsymbol{q}) \mathrm{D}\mathcal{S}(\boldsymbol{q}) = 0$ and $\mathbb{K}(\boldsymbol{q}) \mathrm{D}\mathcal{E}(\boldsymbol{q}) = 0$ hold even true on the level of each individual dissipative process, i.e., heat transport, heat exchange, Stokes dissipation, Darcy dissipation. The Darcy friction is objective and conserves the total momentum. The total mass density of the system evolves according to

$$\partial_t \varrho_{\mathrm{tot}} + \nabla \cdot \varrho_{\mathrm{tot}} \boldsymbol{v} = 0\,, \quad \text{where} \quad \varrho_{\mathrm{tot}} \boldsymbol{v} = \varrho_{\mathrm{s}} \boldsymbol{v}_{\mathrm{s}} + \varrho_{\mathrm{f}} \boldsymbol{v}_{\mathrm{f}}. \tag{2.21}$$

2.2 Two-phase reaction-diffusion system

We now discuss the gradient/Onsager structure of a two-phase system that allows for the diffusion of species and intra-phase as well as inter-phase chemical reactions among the species. For this, we suitably adapt the results of [ZPT21, Sec. 5 & 6.1] to the two-phase setting. For this two-phase system of solid (s) and fluid (f) phase in Eulerian coordinates we consider the state vector $\boldsymbol{q} = (\boldsymbol{q}_{\mathrm{f}}, \boldsymbol{q}_{\mathrm{s}})$ from (2.9). In particular, we assume that the two-phase system is composed of $N = N_{\mathrm{s}} + N_{\mathrm{f}}$ chemical species $Z_1, \dots, Z_N$. Hereby, the first N_{s} species $Z_1, \dots, Z_{N_{\mathrm{s}}}$ belong to the solid phase and the N_{f} species $Z_{N_{\mathrm{s}+1}}, \dots, Z_N$ belong to the fluid phase and we denote by C_k the particle density of species Z_k, $k \in \{1, \dots, N\}$. Accordingly, we set $\boldsymbol{C}_{\mathrm{s}} := (C_1, \dots, C_{N_{\mathrm{s}}})^\top = (C_1^{\mathrm{s}}, \dots, C_{N_{\mathrm{s}}}^{\mathrm{s}})^\top$, $\boldsymbol{C}_{\mathrm{f}} := (C_{N_{\mathrm{s}+1}}, \dots, C_N)^\top = (C_1^{\mathrm{f}}, \dots, C_{N_{\mathrm{f}}}^{\mathrm{f}})^\top$, and $\boldsymbol{C} = (C_1, \dots, C_N)^\top$. The total energy and entropy of the system are of the form (2.11), with the chemical part of the entropy of logarithmic type, i.e., S_i in (2.11b) is of the form

$$S_i(\boldsymbol{C}_i, U_i) := S_i^{\mathrm{th}}(U_i) + \sum_{k=1}^{N_i} C_k^i (\ln C_k^i - 1) \tag{2.22}$$

with $S_i^{\mathrm{th}}(U_i)$ a thermal contribution. This leads to the driving force

$$\mathrm{D}_{\boldsymbol{C}_i} S_i(\boldsymbol{C}_i, U_i) = (\ln C_k^i)_{k=1}^{N_i}\,. \tag{2.23}$$

We further assume that the conservative contribution to dynamics is represented by the operator $\mathbb{J}$ from (2.14). In analogy to (2.15) we introduce the general structure of the Onsager operator for the two-phase reaction-diffusion system as follows

$$\mathbb{K}_{\mathrm{rd}} := \begin{pmatrix} \mathbb{K}_{\mathrm{rd}}^{\mathrm{ss}} & \mathbb{K}_{\mathrm{rd}}^{\mathrm{sf}} \\ \mathbb{K}_{\mathrm{rd}}^{\mathrm{fs}} & \mathbb{K}_{\mathrm{rd}}^{\mathrm{ff}} \end{pmatrix} \text{ with } \mathbb{K}_{\mathrm{rd}}^{ij} := \begin{pmatrix} 0 & 0 & 0 \\ 0 & \mathbb{K}_{\boldsymbol{C}_i \boldsymbol{C}_j} & 0 \\ 0 & 0 & 0 \end{pmatrix} \text{ and } \mathbb{K}_{\boldsymbol{C}_i \boldsymbol{C}_j} := \mathbb{K}_{\boldsymbol{C}_i \boldsymbol{C}_j}^{\mathrm{reac}} + \mathbb{K}_{\boldsymbol{C}_i \boldsymbol{C}_j}^{\mathrm{diff}} \tag{2.24}$$

for $i, j \in \{\mathrm{s}, \mathrm{f}\}$. In this way the operators $\mathbb{K}_{\mathrm{rd}}^{ij}$ only account for dissipative interactions of the vectors of concentrations in terms of chemical reactions $\mathbb{K}_{\boldsymbol{C}_i \boldsymbol{C}_j}^{\mathrm{reac}}$ and diffusion $\mathbb{K}_{\boldsymbol{C}_i \boldsymbol{C}_j}^{\mathrm{diff}}$, whereas dissipation due to changes in

momentum $\boldsymbol{P}_i$ and internal energy U_i is not considered for $i \in \{\mathrm{s},\mathrm{f}\}$. We note that $\mathbb{K}^{\mathrm{reac}}_{\boldsymbol{C}_i\boldsymbol{C}_j}$ describes intra-phase chemical reactions for $i = j$ and inter-phase chemical reactions for $i \neq j$. Following [ZPT21, Eq. (6.9)] we now introduce the Onsager operators $\mathbb{K}^{\mathrm{reac}}_{\boldsymbol{C}_i\boldsymbol{C}_j}$ and $\mathbb{K}^{\mathrm{diff}}_{\boldsymbol{C}_i\boldsymbol{C}_j}$.

Onsager operator for diffusion. Following [ZPT21, Sec. 5 & 6.1] we introduce the Eulerian dual dissipation potential for diffusion

$$\Psi^*_{\mathrm{diff}}(\boldsymbol{q};\boldsymbol{\eta}) := \int_\Omega \tfrac{1}{2}\mathbb{M}_{\boldsymbol{CC}}\nabla\boldsymbol{\eta}{:}\nabla\boldsymbol{\eta}\,\mathrm{d}\boldsymbol{x} \tag{2.25}$$

for any $\boldsymbol{\eta} = (\boldsymbol{\eta}_\mathrm{s},\boldsymbol{\eta}_\mathrm{f}) = (\boldsymbol{\eta}_{\boldsymbol{C}_\mathrm{s}},\boldsymbol{\eta}_{\boldsymbol{C}_\mathrm{f}})$. Differentiation with respect to $\boldsymbol{\eta}$ and integration by parts under the assumption of homogeneous boundary conditions gives the Onsager operator

$$\mathbb{K}^{\mathrm{diff}}\boldsymbol{\eta} = -\nabla\cdot\big(\mathbb{M}_{\boldsymbol{CC}}\nabla\boldsymbol{\eta}\big) \text{ with } \mathbb{M}_{\boldsymbol{CC}} = \begin{pmatrix}\mathbb{M}_{\boldsymbol{C}_\mathrm{s}\boldsymbol{C}_\mathrm{s}} & \mathbb{M}_{\boldsymbol{C}_\mathrm{s}\boldsymbol{C}_\mathrm{f}}\\ \mathbb{M}_{\boldsymbol{C}_\mathrm{f}\boldsymbol{C}_\mathrm{s}} & \mathbb{M}_{\boldsymbol{C}_\mathrm{f}\boldsymbol{C}_\mathrm{f}}\end{pmatrix} \in \mathbb{R}^{N\times N} \tag{2.26}$$

a positively semidefinite matrix of diffusion coefficients, which may depend on the state vector $\boldsymbol{q}$. Comparing (2.26) with (2.24) shows that

$$\mathbb{K}^{\mathrm{diff}}_{\boldsymbol{C}_i\boldsymbol{C}_j}\square = \nabla\cdot\big(\mathbb{M}_{\boldsymbol{C}_i\boldsymbol{C}_j}\nabla\square\big) \text{ with } \mathbb{M}_{\boldsymbol{C}_i\boldsymbol{C}_j} \in \mathbb{R}^{N_i\times N_j} \tag{2.27}$$

and $\square$ indicates where the argument has to be placed.

Onsager operator for chemical reactions. Assume that above N chemical species react with each other in R chemical reactions according to

$$\alpha^r_1 Z_1 + \ldots + \alpha^r_{N^\mathrm{s}} Z_{N^\mathrm{s}} + \alpha^r_{N^\mathrm{s}+1} Z_{N^\mathrm{s}+1} + \ldots + \alpha^r_N Z_N \underset{\mathrm{k}^r_-}{\overset{\mathrm{k}^r_+}{\rightleftharpoons}} \beta^r_1 Z_1 + \ldots + \beta^r_{N^\mathrm{s}} Z_N + \beta^r_{N^\mathrm{s}+1} Z_1 + \ldots + \beta^r_N Z_N\,, \tag{2.28}$$

for $r = 1,\ldots,R$. For each reaction r there are the vectors of stoichiometric coefficients $\boldsymbol{\alpha}^r = (\boldsymbol{\alpha}^r_\mathrm{s},\boldsymbol{\alpha}^r_\mathrm{f}) = (\alpha^r_1,\ldots,\alpha^r_N)$ and $\boldsymbol{\beta}^r = (\boldsymbol{\beta}^r_\mathrm{s},\boldsymbol{\beta}^r_\mathrm{f}) = (\beta^r_1,\ldots,\beta^r_N) \in \mathbb{N}^N_0$, as well as the forward and backward reaction rates $k^r_+, k^r_- > 0$, which may depend on the state $\boldsymbol{q}$. The equations governing the reaction kinetics are given by an ODE system of the form

$$\mathrm{d}^i_t\boldsymbol{C}_i = \sum_{r=1}^R \Big(k^r_-(\boldsymbol{q})\boldsymbol{C}^{\boldsymbol{\beta}^r} - k^r_+(\boldsymbol{q})\boldsymbol{C}^{\boldsymbol{\alpha}^r}\Big)\,(\boldsymbol{\alpha}^r_i - \boldsymbol{\beta}^r_i) \quad \text{for } i \in \{\mathrm{s},\mathrm{f}\}\,, \tag{2.29}$$

where we use the notation $\boldsymbol{C}^\alpha := C^{\alpha_1}_1 \cdots C^{\alpha_N}_N$ and where d^i_t denotes the material time derivative with respect to the velocity of phase i. The material time derivative is generated by $\mathbb{J}$, see (2.20c) & (2.20d). Furthermore, we assume a detailed balance condition, i.e., there exists a steady state $\boldsymbol{C}_\mathrm{ref}$, such that

$$k^r(\boldsymbol{q}) = k^r_+(\boldsymbol{q})\boldsymbol{C}^{\boldsymbol{\alpha}^r}_\mathrm{ref} = k^r_-(\boldsymbol{q})\boldsymbol{C}^{\boldsymbol{\beta}^r}_\mathrm{ref} \text{ for all } r = 1,\ldots,R\,. \tag{2.30}$$

Under this condition the system (2.29) can be written as an Onsager system, cf. e.g. [Mie11]. Based on [ZPT21, Sec. 5] we introduce the dual dissipation potential for chemical reactions

$$\Psi^*_{\mathrm{reac}}(\boldsymbol{q};\boldsymbol{\eta}) := \int_\Omega \tfrac{1}{2}\begin{pmatrix}\boldsymbol{\eta}_\mathrm{s}\\ \boldsymbol{\eta}_\mathrm{f}\end{pmatrix}\cdot\mathbb{H}_{\boldsymbol{CC}}(\boldsymbol{q})\begin{pmatrix}\boldsymbol{\eta}_\mathrm{s}\\ \boldsymbol{\eta}_\mathrm{f}\end{pmatrix}\,\mathrm{d}\boldsymbol{x}\,, \tag{2.31a}$$

with the Onsager operator $\mathbb{H}_{\boldsymbol{CC}}$. Due to (2.23) it follows that the Onsager operator has the following expression

$$\mathbb{H}_{\boldsymbol{CC}}(\boldsymbol{q}) := \sum_{r=1}^{R} \frac{k^r(\boldsymbol{q})}{k_{\mathrm{B}}} \ell\left(\left(\frac{\boldsymbol{C}}{\boldsymbol{C}_{\mathrm{ref}}}\right)^{\boldsymbol{\alpha}^r}, \left(\frac{\boldsymbol{C}}{\boldsymbol{C}_{\mathrm{ref}}}\right)^{\boldsymbol{\beta}^r}\right) \bar{\mathbb{S}}^r\,, \tag{2.31b}$$

$$\bar{\mathbb{S}}^r := (\boldsymbol{\alpha}^r - \boldsymbol{\beta}^r) \otimes (\boldsymbol{\alpha}^r - \boldsymbol{\beta}^r)\,, \tag{2.31c}$$

$$\ell(u,v) := \begin{cases} \frac{u-v}{\log u - \log v} & \text{for } u \neq v\,, \\ v & \text{for } u = v\,. \end{cases} \tag{2.31d}$$

Comparing (2.31b) with (2.24) we gather that

$$\mathbb{H}_{\boldsymbol{CC}}(\boldsymbol{q}) \quad = \quad \begin{pmatrix} \mathbb{K}^{\mathrm{reac}}_{\boldsymbol{C}_{\mathrm{s}}\boldsymbol{C}_{\mathrm{s}}} & \mathbb{K}^{\mathrm{reac}}_{\boldsymbol{C}_{\mathrm{s}}\boldsymbol{C}_{\mathrm{f}}} \\ \mathbb{K}^{\mathrm{reac}}_{\boldsymbol{C}_{\mathrm{f}}\boldsymbol{C}_{\mathrm{s}}} & \mathbb{K}^{\mathrm{reac}}_{\boldsymbol{C}_{\mathrm{f}}\boldsymbol{C}_{\mathrm{f}}} \end{pmatrix} \text{ and} \tag{2.32a}$$

$$\mathbb{K}^{\mathrm{reac}}_{\boldsymbol{C}_i\boldsymbol{C}_j}(\boldsymbol{q}) := \sum_{r=1}^{R} \frac{k^r(\boldsymbol{q})}{k_{\mathrm{B}}} \ell\left(\left(\frac{\boldsymbol{C}}{\boldsymbol{C}_{\mathrm{ref}}}\right)^{\boldsymbol{\alpha}^r}, \left(\frac{\boldsymbol{C}}{\boldsymbol{C}_{\mathrm{ref}}}\right)^{\boldsymbol{\beta}^r}\right) (\boldsymbol{\alpha}_i^r - \boldsymbol{\beta}_i^r) \otimes (\boldsymbol{\alpha}_j^r - \boldsymbol{\beta}_j^r) \text{ for } i,j \in \{\mathrm{s},\mathrm{f}\}\,. \tag{2.32b}$$

Example 2.1 (Rock dehydration)**.** Consider the process of dehydration of serpentinite

$$(\mathrm{Mg},\mathrm{Fe})_3\mathrm{Si}_2\mathrm{O}_5(\mathrm{OH})_4 + (\mathrm{Mg},\mathrm{Fe})(\mathrm{OH})_2 \rightleftharpoons 2(\mathrm{Mg},\mathrm{Fe})_2\mathrm{SiO}_4 + 3\mathrm{H}_2\mathrm{O}$$

as an example for a single reaction in a two phase system with four species corresponding to antigorite $Z_1 = (\mathrm{Mg},\mathrm{Fe})_3\mathrm{Si}_2\mathrm{O}_5(\mathrm{OH})_4$, brucite $Z_2 = (\mathrm{Mg},\mathrm{Fe})(\mathrm{OH})_2$, olivine $Z_3 = (\mathrm{Mg},\mathrm{Fe})_2\mathrm{SiO}_4$ and water $Z_4 = \mathrm{H}_2\mathrm{O}$. Therefore we have the liquid phase composed only by water and the remaining minerals forming the solid part. If we consider purely Mg-minerals then the vector of molecular masses is $\boldsymbol{M} = (277.11, 58.32, 140.69, 18.01)$ expressed in $\mathrm{g/mol}$ with stoichiometric coefficients

$$\begin{aligned} \boldsymbol{\alpha}_{\mathrm{s}} &= (1,1,0)\,, & \boldsymbol{\alpha}_{\mathrm{f}} &= (0)\,, \\ \boldsymbol{\beta}_{\mathrm{s}} &= (0,0,2)\,, & \boldsymbol{\beta}_{\mathrm{f}} &= (3)\,. \end{aligned}$$

Note that conservation of mass is ensured by $\boldsymbol{M}_{\mathrm{s}} \cdot (\boldsymbol{\alpha}_{\mathrm{s}} - \boldsymbol{\beta}_{\mathrm{s}}) + \boldsymbol{M}_{\mathrm{f}} \cdot (\boldsymbol{\alpha}_{\mathrm{f}} - \boldsymbol{\beta}_{\mathrm{f}}) = 0$. Finally, the system of ODEs reads

$$\partial_t \begin{pmatrix} \boldsymbol{C}_1 \\ \boldsymbol{C}_2 \\ \boldsymbol{C}_3 \\ \boldsymbol{C}_4 \end{pmatrix} = k(\boldsymbol{q}) \left(\frac{(\boldsymbol{C}_3)^2 (\boldsymbol{C}_4)^3}{(\boldsymbol{C}_{3,\mathrm{ref}})^2 (\boldsymbol{C}_{4,\mathrm{ref}})^3} - \frac{\boldsymbol{C}_1\boldsymbol{C}_2}{\boldsymbol{C}_{1,\mathrm{ref}}\boldsymbol{C}_{2,\mathrm{ref}}} \right) \begin{pmatrix} 1 \\ 1 \\ -2 \\ -3 \end{pmatrix}$$

⋆

2.3 Two-phase reactive Darcy flow

Here we combine our findings from Sections 2.1 and 2.2 to obtain the GENERIC structure for a two-phase Darcy flow with reactions and diffusion of chemical species. We thus again consider the state vector $\boldsymbol{q}$ from (2.9), the driving functionals $\mathcal{E}$ and $\mathcal{S}$ from (2.11) with the properties of the chemical part of the entropy as in (2.22) and the properties of the chemical species as discussed in Sec. 2.2. The Poisson operator $\mathbb{J}$ for reversible dynamics is again given by (2.14), while the Onsager operator for the coupled dissipative processes results by the sum of $\mathbb{K}_{\mathrm{SDH}}$ from (2.15) and $\mathbb{K}_{\mathrm{rd}}$ from (2.24), i.e.,

$$\mathbb{K}_{\mathrm{rdSDH}} = \mathbb{K}_{\mathrm{rd}} + \mathbb{K}_{\mathrm{SDH}}\,. \tag{2.33}$$

Following the lines of [ZPT21, Sec. 6.1] it can be checked that this choice of driving functionals and operators complies with the degeneracy conditions (2.1) and (2.2). Moreover, the evolution equations of the GENERIC system for the reactive two-phase Darcy flow read

$$\dot{\boldsymbol{P}}_{\mathrm{s}} + \nabla \cdot (\boldsymbol{P}_{\mathrm{s}} \otimes \boldsymbol{v}_{\mathrm{s}}) = -\nabla \pi_{\mathrm{s}} - K_{\mathrm{D}} \boldsymbol{\gamma} + \nabla \cdot \boldsymbol{\sigma}_{\mathrm{s}}\,, \tag{2.34a}$$

$$\dot{\boldsymbol{P}}_{\mathrm{f}} + \nabla \cdot (\boldsymbol{P}_{\mathrm{f}} \otimes \boldsymbol{v}_{\mathrm{f}}) = -\nabla \pi_{\mathrm{f}} + K_{\mathrm{D}} \boldsymbol{\gamma} + \nabla \cdot \boldsymbol{\sigma}_{\mathrm{f}}\,, \tag{2.34b}$$

$$\dot{\boldsymbol{C}}_{\mathrm{s}} + \nabla \cdot (\boldsymbol{C}_{\mathrm{s}} \otimes \boldsymbol{v}_{\mathrm{s}}) = \sum_{r=1}^{R} k^r(\boldsymbol{q}) \left(\boldsymbol{C}^{\boldsymbol{\beta}^r} - \boldsymbol{C}^{\boldsymbol{\alpha}^r} \right) (\boldsymbol{\alpha}_{\mathrm{s}}^r - \boldsymbol{\beta}_{\mathrm{s}}^r)\,, \tag{2.34c}$$

$$\dot{\boldsymbol{C}}_{\mathrm{f}} + \nabla \cdot (\boldsymbol{C}_{\mathrm{f}} \otimes \boldsymbol{v}_{\mathrm{f}}) = \sum_{r=1}^{R} k^r(\boldsymbol{q}) \left(\boldsymbol{C}^{\boldsymbol{\beta}^r} - \boldsymbol{C}^{\boldsymbol{\alpha}^r} \right) (\boldsymbol{\alpha}_{\mathrm{f}}^r - \boldsymbol{\beta}_{\mathrm{f}}^r)\,, \tag{2.34d}$$

$$\dot{U}_{\mathrm{s}} + \nabla \cdot (U_{\mathrm{s}} \boldsymbol{v}_{\mathrm{s}}) = -\pi_{\mathrm{s}} \nabla \cdot \boldsymbol{v}_{\mathrm{s}} + \alpha K_{\mathrm{D}} |\boldsymbol{\gamma}|^2 + k_{\mathrm{he}} (\theta_{\mathrm{s}}^{-1} - \theta_{\mathrm{f}}^{-1}) + \nabla \cdot (k_{\mathrm{s}} \nabla \theta_{\mathrm{s}})\,, \tag{2.34e}$$

$$\dot{U}_{\mathrm{f}} + \nabla \cdot (U_{\mathrm{f}} \boldsymbol{v}_{\mathrm{f}}) = -\pi_{\mathrm{f}} \nabla \cdot \boldsymbol{v}_{\mathrm{f}} + (1-\alpha) K_{\mathrm{D}} |\boldsymbol{\gamma}|^2 - k_{\mathrm{he}} (\theta_{\mathrm{s}}^{-1} - \theta_{\mathrm{f}}^{-1}) + \nabla \cdot (k_{\mathrm{f}} \nabla \theta_{\mathrm{f}})\,. \tag{2.34f}$$

Our deduction shows that the two-phase system (2.34) has a GENERIC structure. This in particular brings about that each phase has its own individual internal energy, entropy, and temperature. It is our goal to show that the porous-media models (1.1) and (1.2) result from system (2.34) and its GENERIC structure. For this we shall investigate the limit to a joint system's temperature by assuming that heat can be equilibrated infinitely fast throughout the phases. In addition we will assume that the chemical reactions take place on much faster time scales than diffusion and Darcy flow. To this end we subsequently study on a formal level the equilibration of fast dissipative processes within the GENERIC framework.

3 Equilibration of fast dissipative processes

We consider GENERIC systems of the form

$$\dot{\boldsymbol{q}} = \mathbb{J}(\boldsymbol{q}) \mathrm{D}\mathcal{E}(\boldsymbol{q}) + \mathbb{K}(\boldsymbol{q}) \mathrm{D}\mathcal{S}(\boldsymbol{q}) \tag{3.1a}$$

where the irreversible processes encoded in $\mathbb{K}$ are of the form

$$\mathbb{K}(\boldsymbol{q}) = \mathbb{K}_{\mathrm{slow}}(\boldsymbol{q}) + \varepsilon^{-1} \mathbb{K}_{\mathrm{fast}}(\boldsymbol{q}), \tag{3.1b}$$

and where $\mathbb{J}, \mathbb{K}$ satisfy the usual conditions of a GENERIC system. The NIC for $\mathbb{K}$ is satisfied for slow and fast processes separately, i.e., $\mathbb{K}_{\mathrm{slow}}(\boldsymbol{q}) \mathrm{D}\mathcal{E}(\boldsymbol{q}) = 0$ and $\mathbb{K}_{\mathrm{fast}}(\boldsymbol{q}) \mathrm{D}\mathcal{E}(\boldsymbol{q}) = 0$. We are interested in deriving the effective dynamics for solutions $\boldsymbol{q} : [0, \mathsf{T}] \to \mathcal{Q}$ of (3.1) as $\varepsilon \to 0$. Based on the considerations in previous sections, we are interested in two particular cases, i.e., the limit of fast exchange of thermal energy and the limit of fast reactions. In the following we present two possible approaches based on considerations in [MPS21, ZPT21] that are closely linked to the Gibbs-minimization formalism described in [BPL82].

3.1 Fast exchange of thermal energy

We consider a GENERIC system where energy and entropy are of the form

$$\mathcal{E}(\boldsymbol{q}) = \int_{\Omega} \frac{|\boldsymbol{P}_{\mathrm{s}}|^2}{2\varrho_{\mathrm{s}}} + \frac{|\boldsymbol{P}_{\mathrm{f}}|^2}{2\varrho_{\mathrm{f}}} + U_{\mathrm{s}} + U_{\mathrm{f}} \,\mathrm{d}\boldsymbol{x}\,, \tag{3.2a}$$

$$\mathcal{S}(\boldsymbol{q}) = \int_{\Omega} S_{\mathrm{s}}(\hat{q}, U_{\mathrm{s}}) + S_{\mathrm{f}}(\hat{q}, U_{\mathrm{f}}) \,\mathrm{d}\boldsymbol{x}\,, \tag{3.2b}$$

and we write $\boldsymbol{q} = (\boldsymbol{P}_\mathrm{s}, \boldsymbol{P}_\mathrm{f}, \dots, U_\mathrm{s}, U_\mathrm{f}) \equiv (\hat{q}, U_\mathrm{s}, U_\mathrm{f})$. To simplify the notation for the next consideration we introduced $\hat{q}$, which contains all state variables except for the internal energies.

Remark 3.1. Note that S_i for $i \in \{\mathrm{s}, \mathrm{f}\}$ does not depend on the momentum and that the entropy of one phase does not depend on any variables of the other phase. While this structural assumption might be quite restrictive and prevent entropies that feature interaction between phases such as in the Flory-Huggins theory [Flo42, Hug41], this is necessary in order to guarantee the non-interaction condition $\mathbb{J}(\boldsymbol{q})\mathrm{D}\mathcal{S}(\boldsymbol{q}) = 0$ for $\mathbb{J}$ in the current form. In general, Flory-Huggins theory features phase-separation via a non-concave entropy, which we also exclude here.

Corresponding to this 3-component representation of the state variable $\boldsymbol{q} = (\hat{q}, U_\mathrm{s}, U_\mathrm{f})$, we consider fast processes of the form

$$\mathbb{K}_\mathrm{fast} = \begin{pmatrix} 0 & 0 & 0 \\ 0 & +1 & -1 \\ 0 & -1 & +1 \end{pmatrix}, \tag{3.3}$$

without any dependence on $\boldsymbol{q}$. Due to $\mathrm{D}\mathcal{E}(\boldsymbol{q}) = (\mathrm{D}_{\hat{q}}\mathcal{E}(\boldsymbol{q}), 1, 1)^\top$ we satisfy the NIC for the fast processes, i.e., $\mathbb{K}_\mathrm{fast}\mathrm{D}\mathcal{E}(\boldsymbol{q}) = 0$. Then fast exchange of thermal energy is equivalent to the requirement

$$\xi_{U_\mathrm{s}} = \mathrm{D}_{U_\mathrm{s}}\mathcal{S}(\boldsymbol{q}) \overset{!}{=} \mathrm{D}_{U_\mathrm{f}}\mathcal{S}(\boldsymbol{q}) = \xi_{U_\mathrm{f}}\,, \tag{3.4}$$

which correspondingly gives us the linear system with Lagrange multipliers

$$\dot{\boldsymbol{q}} = \begin{pmatrix} \dot{\hat{q}} \\ \dot{U}_\mathrm{s} \\ \dot{U}_\mathrm{f} \end{pmatrix} = \mathbb{J}(\boldsymbol{q})\mathrm{D}\mathcal{E}(\boldsymbol{q}) + \mathbb{K}_\mathrm{slow}(\boldsymbol{q})\mathrm{D}\mathcal{S}(\boldsymbol{q}) + \underbrace{\begin{pmatrix} \hat{0} \\ +\lambda \\ -\lambda \end{pmatrix}}_{=:\Lambda}, \tag{3.5a}$$

$$0 = \mathrm{D}_{U_\mathrm{s}}\mathcal{S}(\boldsymbol{q}) - \mathrm{D}_{U_\mathrm{f}}\mathcal{S}(\boldsymbol{q}) \equiv \theta_\mathrm{s}^{-1} - \theta_\mathrm{f}^{-1}. \tag{3.5b}$$

The advantage of the formulation *with Lagrange multipliers* is that it is directly accessible from the full model, but it has the disadvantage of increasing the number of unknowns.

Remark 3.2 (NIC for effective dynamics)**.** Using the chain rule we have

$$\begin{aligned} \frac{\mathrm{d}}{\mathrm{d}t}\mathcal{E}(\boldsymbol{q}(t)) &= \langle \mathrm{D}\mathcal{E}(\boldsymbol{q}), \Lambda\rangle \equiv 0, \\ \frac{\mathrm{d}}{\mathrm{d}t}\mathcal{S}(\boldsymbol{q}(t)) &= \underbrace{\langle \mathrm{D}\mathcal{S}(\boldsymbol{q}), \mathbb{K}_\mathrm{slow}(\boldsymbol{q})\mathrm{D}\mathcal{S}(\boldsymbol{q})\rangle}_{\geq 0} + \underbrace{\langle \mathrm{D}\mathcal{S}(\boldsymbol{q}), \Lambda\rangle}_{=0} \geq 0\,. \end{aligned}$$

This shows that the effective dynamics complies with thermodynamic consistency.

The system (3.5) with Lagrange multipliers presents one possibility to write the fast thermal equilibration limit of the general evolution. Alternatively, we can define the simple transformation

$$\mathrm{T}_U(\boldsymbol{q}) \equiv (\hat{q}, U = U_\mathrm{s} + U_\mathrm{f}) = \tilde{\boldsymbol{q}}, \tag{3.6}$$

which, using (3.4), is invertible on the set that also satisfies (3.4). If we define

$$\tilde{\mathcal{S}}(\tilde{\boldsymbol{q}}) := \mathcal{S}(\mathrm{T}_U^{-1}(\tilde{\boldsymbol{q}})), \qquad \tilde{\mathcal{E}}(\tilde{\boldsymbol{q}}) := \mathcal{E}(\mathrm{T}_U^{-1}(\tilde{\boldsymbol{q}})),$$

and using $\mathbb{L}_U = \mathrm{D}\mathrm{T}_U(\boldsymbol{q})$ gives the transformed evolution

$$\tilde{\mathbb{J}}(\tilde{\boldsymbol{q}}) = \mathbb{L}_U\, \mathbb{J}(\mathrm{T}_U^{-1}(\tilde{\boldsymbol{q}}))\, \mathbb{L}_U^*,$$
$$\tilde{\mathbb{K}}_{\mathrm{slow}}(\tilde{\boldsymbol{q}}) = \mathbb{L}_U\, \mathbb{K}_{\mathrm{slow}}(\mathrm{T}_U^{-1}(\tilde{\boldsymbol{q}}))\, \mathbb{L}_U^*,$$

governing the reduced dynamics for $\theta_{\mathrm{s}} = \theta_{\mathrm{f}} = \theta$ via

$$\dot{\tilde{\boldsymbol{q}}} = \tilde{\mathbb{J}}(\tilde{\boldsymbol{q}})\mathrm{D}\tilde{\mathcal{E}}(\tilde{\boldsymbol{q}}) + \tilde{\mathbb{K}}_{\mathrm{slow}}(\tilde{\boldsymbol{q}})\mathrm{D}\tilde{\mathcal{S}}(\tilde{\boldsymbol{q}}). \tag{3.7}$$

We give a simple ODE example, which shows how this reduction can be performed in more detail.

Example 3.3 (Fast thermal equilibration ODE)**.** Consider $\boldsymbol{q} = (x_1, x_2, p_1, p_2, u_1, u_2) \in \mathbb{R}^6$ as state variable, where x_i denotes position, p_i the momentum, and u_i the internal energy of the components/phases $i \in \{1, 2\}$. The total energy E and entropy S of the system are

$$E(\boldsymbol{q}) = \sum_i \frac{p_i^2}{2m_i} + u_i, \qquad S(\boldsymbol{q}) = \sum_i S_i(x_i, u_i),$$

using the entropy $S_i(x_i, u_i)$ for each separate phase and with the Gibbs relations $\partial_{u_i} S_i = 1/\theta_i$ and $\partial_{x_i} S_i = \pi_i/\theta_i$ defining temperature θ_i and pressure π_i. Consider the GENERIC system

$$\dot{\boldsymbol{q}} = \mathbb{J}(\boldsymbol{q})\mathrm{D}E(\boldsymbol{q}) + \mathbb{K}(\boldsymbol{q})\mathrm{D}S(\boldsymbol{q}), \tag{3.8a}$$

where the GENERIC structure is defined and NIC $\mathbb{J}(\boldsymbol{q})\mathrm{D}\mathcal{S}(\boldsymbol{q}) = 0$ satisfied by using

$$\mathbb{J}(\boldsymbol{q}) = \begin{pmatrix} 0 & 0 & 1 & 0 & 0 & 0 \\ 0 & 0 & 0 & 1 & 0 & 0 \\ -1 & 0 & 0 & 0 & \pi_1 & 0 \\ 0 & -1 & 0 & 0 & 0 & \pi_2 \\ 0 & 0 & -\pi_1 & 0 & 0 & 0 \\ 0 & 0 & 0 & -\pi_2 & 0 & 0 \end{pmatrix}, \quad \mathrm{D}E(\boldsymbol{q}) = \begin{pmatrix} 0 \\ 0 \\ \frac{p_1}{m_1} \\ \frac{p_2}{m_2} \\ 1 \\ 1 \end{pmatrix}, \quad \mathrm{D}S(\boldsymbol{q}) = \begin{pmatrix} \pi_1/\theta_1 \\ \pi_2/\theta_2 \\ 0 \\ 0 \\ 1/\theta_1 \\ 1/\theta_2 \end{pmatrix}. \tag{3.8b}$$

For the dissipation $\mathbb{K}(\boldsymbol{q}) = \mathbb{K}_{\mathrm{slow}}(\boldsymbol{q}) + \varepsilon^{-1}\mathbb{K}_{\mathrm{fast}}(\boldsymbol{q})$ and with $m_i v_i = p_i$ we use

$$\mathbb{K}_{\mathrm{slow}}(\boldsymbol{q}) = \theta_1 k_1 \begin{pmatrix} 0&0 & 0 & 0 & 0 & 0 \\ 0&0 & 0 & 0 & 0 & 0 \\ 0&0 & 1 & 0 & -v_1 & 0 \\ 0&0 & 0 & 0 & 0 & 0 \\ 0&0 & -v_1 & 0 & +v_1^2 & 0 \\ 0&0 & 0 & 0 & 0 & 0 \end{pmatrix} + \theta_2 k_2 \begin{pmatrix} 0&0&0 & 0 & 0 & 0 \\ 0&0&0 & 0 & 0 & 0 \\ 0&0&0 & 0 & 0 & 0 \\ 0&0&0 & 1 & 0 & -v_2 \\ 0&0&0 & 0 & 0 & 0 \\ 0&0&0 & -v_2 & 0 & +v_2^2 \end{pmatrix}, \qquad \mathbb{K}_{\mathrm{fast}} = \begin{pmatrix} 0&0&0&0&0 & 0 & 0 \\ 0&0&0&0&0 & 0 & 0 \\ 0&0&0&0&0 & 0 & 0 \\ 0&0&0&0&0 & 0 & 0 \\ 0&0&0&0&0 & +1 & -1 \\ 0&0&0&0&0 & -1 & +1 \end{pmatrix}, \tag{3.8c}$$

and observe that it satisfies the other NIC $\mathbb{K}(\boldsymbol{q})\mathrm{D}E(\boldsymbol{q}) = 0$. We obtain the following evolution equations

$$\dot{x}_i = v_i = \frac{p_i}{m_i}, \qquad \dot{p}_i = \pi_i - k_i v_i, \tag{3.9a}$$
$$\dot{u}_1 = -\pi_1 v_1 + k_1 v_1^2 + \varepsilon^{-1}(\theta_1^{-1} - \theta_2^{-1}), \tag{3.9b}$$
$$\dot{u}_2 = -\pi_2 v_2 + k_2 v_2^2 + \varepsilon^{-1}(\theta_2^{-1} - \theta_1^{-1}), \tag{3.9c}$$

for $i \in \{1, 2\}$. We introduce an oscillator with $\omega_i \in \mathbb{R}_+$ and heat capacities $c_i \in \mathbb{R}_+$ such that

$$S_i(x_i, u_i) = c_i \log(\tfrac{u_i - V_i(x_i)}{c_i}) = c_i \log \theta_i, \qquad V_i(x_i) = \tfrac{1}{2}\omega_i x_i^2,$$

so that $c_i\theta_i = u_i - V_i(x)$ and $\pi_i = -\partial_x V_i$. Using $\theta_1 = \theta_2 \equiv \theta$, for the total internal energy we get $u = u_1 + u_2 = (c_1 + c_2)\theta + V_1(x_1) + V_2(x_2)$. Correspondingly, the energy $\tilde{E}$ and entropy $\tilde{S} = S_1 + S_2$ can be expressed in $\tilde{\boldsymbol{q}} = (x_1, x_2, p_1, p_2, u) \in \mathbb{R}^5$ with

$$\tilde{E}(\tilde{\boldsymbol{q}}) = \tfrac{p_1^2}{2m_1} + \tfrac{p_2^2}{2m_2} + u, \qquad \tilde{S}(x_1, x_2, u) = (c_1 + c_2)\log\left(\tfrac{u - V_1(x_1) - V_2(x_2)}{(c_1 + c_2)}\right). \tag{3.10a}$$

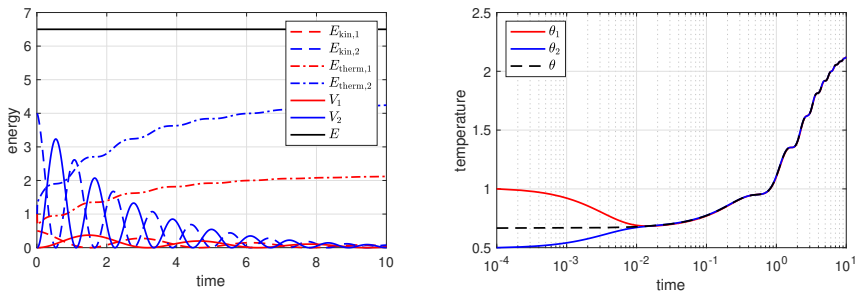

Figure 2: Solution of GENERIC system (3.9) with $\varepsilon = 10^{-2}$ and $k_1 = k_2 = 1/5$, $m_1 = 1$, $m_2 = 1/2$, $c_1 = 1$, $c_2 = 2$, $\omega_1 = 1$, $\omega_2 = 4$ with $\boldsymbol{q}(t=0) = (0,0,1,-2,1,1)^\top$ and $\tilde{\boldsymbol{q}}(t=0) = (0,0,1,-2,2)^\top$. Numerical solution showing (left) kinetic energy $E_{\mathrm{kin},i} = p_i^2/2m_i$, thermal energy $E_{\mathrm{therm},i} = c_i\theta_i = u_i - V_i$, potential energy V_i and total energy E and (right) temperatures of full model θ_i and effective model θ.

Note that $\tilde{S}$ is not a sum of contributions from both components. Using the operators

$$\tilde{\mathbb{J}} = \begin{pmatrix} 0 & 0 & 1 & 0 & 0 \\ 0 & 0 & 0 & 1 & 0 \\ -1 & 0 & 0 & 0 & \pi_1 \\ 0 & -1 & 0 & 0 & \pi_2 \\ 0 & 0 & -\pi_1 & -\pi_2 & 0 \end{pmatrix}, \qquad \tilde{\mathbb{K}}_{\mathrm{slow}} = \theta k_1 \begin{pmatrix} 0 & 0 & 0 & 0 & 0 \\ 0 & 0 & 0 & 0 & 0 \\ 0 & 0 & 1 & 0 & -v_1 \\ 0 & 0 & 0 & 0 & 0 \\ 0 & 0 & -v_1 & 0 & +v_1^2 \end{pmatrix} + \theta k_2 \begin{pmatrix} 0 & 0 & 0 & 0 & 0 \\ 0 & 0 & 0 & 0 & 0 \\ 0 & 0 & 0 & 0 & 0 \\ 0 & 0 & 0 & 1 & -v_2 \\ 0 & 0 & 0 & -v_2 & +v_2^2 \end{pmatrix}, \tag{3.10b}$$

the effective dynamics is $\dot{\tilde{\boldsymbol{q}}} = \tilde{\mathbb{J}}(\tilde{\boldsymbol{q}})\mathrm{D}\tilde{E}(\tilde{\boldsymbol{q}}) + \tilde{\mathbb{K}}_{\mathrm{slow}}(\tilde{\boldsymbol{q}})\mathrm{D}\tilde{S}(\tilde{\boldsymbol{q}})$. An exemplary solution is shown in Fig. 2, where the left panel shows the energetics of the full solution $\boldsymbol{q}(t)$, and the right panel shows the convergence of the temperatures θ_i to the temperature θ of the effective solution $\tilde{\boldsymbol{q}}(t)$.

⋆

3.2 Fast reactions equilibrium

Similar to what is presented in [MPS21], we apply now the aforementioned method to systems where fast chemical reactions happen on a very short time scale compared to the other involved slow processes. In this case, however, it is not necessary to distinguish between a solid and a liquid phase, but rather between the species involved.

Consider a system where R possible reactions with stoichiometric coefficients $\boldsymbol{\alpha}^r, \boldsymbol{\beta}^r \in \mathbb{N}_0^N$ between N species occur. The particle density is denoted by the N-tuple $\boldsymbol{C} = (\boldsymbol{C}_i)_{i=1}^N$. We assume that the total energy and total entropy of the system can be expressed in the following way

$$\mathcal{E}(\boldsymbol{q}) = \int_\Omega \frac{|\boldsymbol{P}|^2}{2\varrho} + U \,\mathrm{d}\boldsymbol{x} \tag{3.11a}$$

$$\mathcal{S}(\boldsymbol{q}) = \int_\Omega S(\hat{q}, \boldsymbol{C}) \,\mathrm{d}\boldsymbol{x}\,, \tag{3.11b}$$

where $\boldsymbol{q} = (\boldsymbol{P}, U, \boldsymbol{C}) \equiv (\hat{q}, \boldsymbol{C})$ with U being the internal energy of the system and $\boldsymbol{P}$ the momentum density. We consider fast processes of the form

$$\mathbb{K}_{\mathrm{fast}} = \begin{pmatrix} 0 & 0 \\ 0 & \mathbb{H} \end{pmatrix}, \tag{3.12}$$

where $\mathbb{H} = \sum_r (\boldsymbol{\alpha}^r - \boldsymbol{\beta}^r) \otimes (\boldsymbol{\alpha}^r - \boldsymbol{\beta}^r)$ is the reactive operator. In order to have mass conservation and to satisfy the NIC, we require that the vector of particle masses $\boldsymbol{M}$ lies in the kernel of the matrix $\mathbb{H}$, i.e.,

$\boldsymbol{M} \cdot (\boldsymbol{\alpha}^r - \boldsymbol{\beta}^r) = 0$ for all reactions $r = 1, \dots, R$. Then a fast reactions limit is equivalent to the equilibrium condition

$$(\boldsymbol{\alpha}^r - \boldsymbol{\beta}^r) \cdot \mathrm{D}_{\boldsymbol{C}} \mathcal{S}(\boldsymbol{q}) \stackrel{!}{=} 0\,, \qquad \text{for all } r \in \{1, \dots, R\}\,, \tag{3.13}$$

Introducing the constrained dynamics by using Lagrange multipliers λ_r, the effective dynamics can be written as

$$\dot{\boldsymbol{q}} = \begin{pmatrix} \dot{\hat{q}} \\ \dot{\boldsymbol{C}} \end{pmatrix} = \mathbb{J}(\boldsymbol{q}) \mathrm{D}\mathcal{E}(\boldsymbol{q}) + \mathbb{K}_{\mathrm{slow}}(\boldsymbol{q}) \mathrm{D}\mathcal{S}(\boldsymbol{q}) + \underbrace{\begin{pmatrix} 0 \\ \sum_r (\boldsymbol{\alpha}^r - \boldsymbol{\beta}^r) \lambda_r \end{pmatrix}}_{:=\Lambda}, \tag{3.14a}$$

$$0 = (\boldsymbol{\alpha}^r - \boldsymbol{\beta}^r) \mathrm{D}_{\boldsymbol{C}} \mathcal{S}(\boldsymbol{q}) \qquad \text{for all } r \in \{1, \dots, R\}\,. \tag{3.14b}$$

Remark 3.4 (NIC for effective dynamics)**.** Similarly as in Remark 3.2, one confirms that the total energy is conserved and entropy is non-decreasing:

$$\frac{\mathrm{d}}{\mathrm{d}t} \mathcal{E}(\boldsymbol{q}(t)) = \langle \mathrm{D}\mathcal{E}(\boldsymbol{q}), \Lambda \rangle \equiv 0\,, \tag{3.15}$$

$$\frac{\mathrm{d}}{\mathrm{d}t} \mathcal{S}(\boldsymbol{q}(t)) = \underbrace{\langle \mathrm{D}\mathcal{S}(\boldsymbol{q}), \mathbb{K}_{\mathrm{slow}}(\boldsymbol{q}) \mathrm{D}\mathcal{S}(\boldsymbol{q}) \rangle}_{\geq 0} + \underbrace{\langle \mathrm{D}\mathcal{S}(\boldsymbol{q}), \Lambda \rangle}_{=0} \geq 0\,, \tag{3.16}$$

where we have used $\boldsymbol{M} \cdot (\boldsymbol{\alpha}^r - \boldsymbol{\beta}^r) = 0$.

The constrained system (3.14a) presents one way to write the fast reactions limit. Another possibility is to define a transformation T_C that reduces the number of variables based on the condition (3.13). In order to build this transformation we use the method presented in [MPS21], similar to the reduction presented [ZPT21]. We start by considering the space

$$\Gamma := \mathrm{span}\,\{\boldsymbol{\alpha}^r - \boldsymbol{\beta}^r | r = 1, \dots, R\} \subset \mathbb{R}^N, \tag{3.17}$$

and its orthogonal complement $\Gamma^\perp$. After finding a basis $\{v_1, \dots, v_m\}$ of $\Gamma^\perp$, we construct the adjoint of the transformation Q as $Q^\top = (v_1, \dots, v_m) \in \mathbb{R}^{N \times m}$. Finally the transformation can be defined as

$$\mathrm{T}_{\boldsymbol{C}}(\boldsymbol{q}) \equiv (\hat{q}, \boldsymbol{C}^\perp = Q\boldsymbol{C}) = \tilde{\boldsymbol{q}}, \tag{3.18}$$

which is invertible on the set defined by (3.13). We define

$$\tilde{\mathcal{E}}(\tilde{\boldsymbol{q}}) := \mathcal{E}(\mathrm{T}_{\boldsymbol{C}}^{-1}(\tilde{\boldsymbol{q}}))\,, \qquad \tilde{\mathcal{S}}(\tilde{\boldsymbol{q}}) := \mathcal{S}(\mathrm{T}_{\boldsymbol{C}}^{-1}(\tilde{\boldsymbol{q}}))\,, \tag{3.19}$$

and set $\mathbb{L}_{\boldsymbol{C}} = \mathrm{D}\mathrm{T}_{\boldsymbol{C}}(\boldsymbol{q})$. This gives the transformed operators

$$\tilde{\mathbb{J}}(\tilde{\boldsymbol{q}}) = \mathbb{L}_{\boldsymbol{C}}\, \mathbb{J}(\mathrm{T}_{\boldsymbol{C}}^{-1}(\tilde{\boldsymbol{q}}))\, \mathbb{L}_{\boldsymbol{C}}^*, \tag{3.20a}$$

$$\tilde{\mathbb{K}}_{\mathrm{slow}}(\tilde{\boldsymbol{q}}) = \mathbb{L}_{\boldsymbol{C}}\, \mathbb{K}_{\mathrm{slow}}(\mathrm{T}_{\boldsymbol{C}}^{-1}(\tilde{\boldsymbol{q}}))\, \mathbb{L}_{\boldsymbol{C}}^*, \tag{3.20b}$$

governing the reduced dynamics for $(\boldsymbol{\alpha}^r - \boldsymbol{\beta}^r) \cdot \boldsymbol{\mu} = 0$ for every $r \in \{1, \dots, R\}$ via

$$\dot{\tilde{\boldsymbol{q}}} = \tilde{\mathbb{J}}(\tilde{\boldsymbol{q}}) \mathrm{D}\tilde{\mathcal{E}}(\tilde{\boldsymbol{q}}) + \tilde{\mathbb{K}}_{\mathrm{slow}}(\tilde{\boldsymbol{q}}) \mathrm{D}\tilde{\mathcal{S}}(\tilde{\boldsymbol{q}}).$$

Note that the determination of effective equations of state $\tilde{E}(\tilde{\boldsymbol{q}})$, $\tilde{S}(\tilde{\boldsymbol{q}})$ and derived quantities is similar to that in the Gibbs minimization process, e.g. cf. [BPL82], which in general is performed for non-convex potentials with the goal to determine the possible phases a mixture attains under the constraint of a prescribed composition of materials.

We now give an explicit example on how the reduction approach can be applied to rock dehydration processes.

Example 3.5 (Fast reactions equilibration for rock dehydration processes.)**.** Consider the following process where water chemically bound to a rock is released

$$\text{hydrous solid} \;\rightleftharpoons\; \text{non-hydrous solid} + \mathrm{H_2O}\,,$$

and the state $\boldsymbol{q} = (U, \boldsymbol{C})^\top = (U, C_{\mathrm{s,h}}, C_{\mathrm{s,nh}}, C_{f,\mathrm{H_2O}})^\top \equiv (u, C_1, C_2, C_{\mathrm{f}})^\top$ with $C_{\mathrm{s,h}}$ and $C_{\mathrm{s,nh}}$ being the concentrations of the hydrous and non-hydrous solid respectively, and u the internal energy. The stoichiometric coefficients for forward and backward reactions are $\boldsymbol{\alpha} = (1,0,0)^\top$ and $\boldsymbol{\beta} = (0,1,1)^\top$ and the vector of particle masses $\boldsymbol{M} = (M_1, M_2, M_{\mathrm{f}})^\top$, with $M_2 = M_1 - M_{\mathrm{f}}$. One can see immediately that $(\boldsymbol{\alpha}-\boldsymbol{\beta})\cdot\boldsymbol{M} = 0$ and thus the condition for conservation of mass is satisfied. For this example we focus only on dissipative processes but the transformation we are going to show applies in the same way to the reversible contributions. Consider then the following Onsager system

$$\partial_t \boldsymbol{q} = \left(\mathbb{K}_{\mathrm{slow}}(\boldsymbol{q}) + \tfrac{1}{\varepsilon}\mathbb{K}_{\mathrm{fast}}(\boldsymbol{q})\right) \mathrm{D}\mathcal{S}(\boldsymbol{q})\,,$$

where

$$\mathbb{K}_{\mathrm{slow}} = \begin{pmatrix} \mathbb{K}_{uu} & \mathbb{K}_{u1} & \mathbb{K}_{u2} & \mathbb{K}_{u\mathrm{f}} \\ \mathbb{K}_{1u} & \mathbb{K}_{11} & \mathbb{K}_{12} & \mathbb{K}_{1\mathrm{f}} \\ \mathbb{K}_{2u} & \mathbb{K}_{21} & \mathbb{K}_{22} & \mathbb{K}_{2\mathrm{f}} \\ \mathbb{K}_{\mathrm{f}u} & \mathbb{K}_{\mathrm{f}1} & \mathbb{K}_{\mathrm{f}2} & \mathbb{K}_{\mathrm{ff}} \end{pmatrix}, \qquad \mathbb{K}_{\mathrm{fast}} = \begin{pmatrix} 0 & 0_{1\times 3} \\ 0_{3\times 1} & \mathbb{H} \end{pmatrix}.$$

The total entropy is of Boltzmann type and has the typical "log" structure

$$\mathcal{S}(\boldsymbol{q}) = \int_\Omega \sum_i C_i^*(u^{\mathrm{s}})\lambda_{\mathrm{B}}\left(\frac{C_i}{C_i^*}\right)\mathrm{d}\boldsymbol{x} \qquad \text{where } \lambda_{\mathrm{B}}(y) := y\log y - y + 1\,,$$

and where $\boldsymbol{C}^*(u) = (C_1^*(u), C_2^*(u), C_{\mathrm{f}}^*(u))^\top$ is the vector of positive concentrations related to the detailed-balance condition. We can directly compute the driving force

$$\mathrm{D}_u\mathcal{S} = \frac{1}{\theta}\,, \qquad (\mathrm{D}_{\boldsymbol{C}}\mathcal{S})_i = \left(\frac{\mu}{\theta}\right)_i = \log C_i/C_i^*\,.$$

The reduction Q is build from a basis of the orthogonal space of $\mathrm{span}\,\{\boldsymbol{\alpha}-\boldsymbol{\beta}\}$

$$Q = \begin{pmatrix} M_1 & M_2 & M_{\mathrm{f}} \\ M_2 & M_2 & 0 \end{pmatrix}.$$

Combining Q with the identity for u we define the nonlinear mapping

$$\tilde{\boldsymbol{q}} := \mathrm{T}_{\boldsymbol{C}}(\boldsymbol{q}) = (u, Q\boldsymbol{C}) = (u, \varrho_{\mathrm{tot}}, \varrho_{\mathrm{nv}})^\top\,,$$

where ϱ_{nv} is the mass density of the non-volatile solid, meaning the mass density of the solid that has no chemically bound water. In order to find out the transformed Onsager operator we need to linearize $\mathrm{T}_{\boldsymbol{C}}$ and compute its adjoint:

$$\mathbb{L}_{\boldsymbol{C}} := \mathrm{D}\mathrm{T}_{\boldsymbol{C}} = \begin{pmatrix} 1 & 0 & 0 & 0 \\ 0 & M_1 & M_2 & M_{\mathrm{f}} \\ 0 & M_2 & M_2 & 0 \end{pmatrix}, \qquad \mathbb{L}_{\boldsymbol{C}}^* = \begin{pmatrix} 1 & 0 & 0 \\ 0 & M_1 & M_2 \\ 0 & M_2 & M_2 \\ 0 & M_{\mathrm{f}} & 0 \end{pmatrix}.$$

The transformed Onsager operator is then given by (3.20b)

$$\mathbb{L}\mathbb{K}(\boldsymbol{q})\mathbb{L}^* = \begin{pmatrix} \mathbb{K}_{uu} & \sum_{\mathrm{i}\in\{1,2,\mathrm{f}\}} \mathbb{K}_{u\mathrm{i}} M_{\mathrm{i}} & \mathbb{K}_{u1}M_1 + \mathbb{K}_{u2}M_2 \\ \sum_{\mathrm{i}\in\{1,2,\mathrm{f}\}} M_{\mathrm{i}}\mathbb{K}_{\mathrm{i}u} & \sum_{i,j\in\{1,2,\mathrm{f}\}} M_i\mathbb{K}_{ij}M_j & \sum_{\mathrm{i}\in\{1,2,\mathrm{f}\}} M_i(\mathbb{K}_{\mathrm{i}1} + \mathbb{K}_{\mathrm{i}2})M_2 \\ M_2\mathbb{K}_{1u} + M_2\mathbb{K}_{2u} & \sum_{\mathrm{i}\in\{1,2,\mathrm{f}\}} M_2(\mathbb{K}_{1\mathrm{i}} + \mathbb{K}_{2\mathrm{i}})M_{\mathrm{i}} & \sum_{\mathrm{i,j}\in\{1,2\}} M_2\mathbb{K}_{\mathrm{ij}}M_2 \end{pmatrix}.$$

This transformed operator and the entropy functional have to satisfy the conditions (3.20) and (3.19), respectively. One can see that it is verified by using $\mathrm{T}_{\boldsymbol{C}}^{-1}$. On the set where the equilibrium condition, i.e., $\mu_1 = \mu_2 + \mu_{\mathrm{f}}$, is satisfied the transformation $\mathrm{T}_{\boldsymbol{C}}$ is invertible and we can reconstruct the vector of concentrations via $\boldsymbol{C} = \mathrm{T}_{\boldsymbol{C}}^{-1}(\tilde{\boldsymbol{q}})$

$$\begin{aligned} C_1 &= \frac{1}{2}\left[K^* + \frac{\varrho_{\mathrm{nv}}}{M_{\mathrm{nv}}} + \frac{\varrho_{\mathrm{tot}} - \varrho_{\mathrm{nv}}}{M_{\mathrm{H_2O}}} - \sqrt{f(u, \varrho_{\mathrm{tot}}, \varrho_{\mathrm{nv}})}\right], \qquad \text{with } K^* := \frac{C^*_{\mathrm{nh}} C^*_{\mathrm{H_2O}}}{C^*_h}, \\ C_2 &= \frac{\varrho_{\mathrm{nv}}}{M_{\mathrm{nh}}} - \frac{1}{2}\left[K^* + \frac{\varrho_{\mathrm{nv}}}{M_{\mathrm{nv}}} + \frac{\varrho_{\mathrm{tot}} - \varrho_{\mathrm{nv}}}{M_{\mathrm{H_2O}}} - \sqrt{f(u, \varrho_{\mathrm{tot}}, \varrho_{\mathrm{nv}})}\right], \\ C_{\mathrm{f}} &= \frac{\varrho_{\mathrm{tot}} - \varrho_{\mathrm{nv}}}{M_{\mathrm{H_2O}}} - \frac{1}{2}\left[K^* + \frac{\varrho_{\mathrm{nv}}}{M_{\mathrm{nv}}} + \frac{\varrho_{\mathrm{tot}} - \varrho_{\mathrm{nv}}}{M_{\mathrm{H_2O}}} - \sqrt{f(u, \varrho_{\mathrm{tot}}, \varrho_{\mathrm{nv}})}\right], \\ \text{with } f(u, \varrho_{\mathrm{tot}}, \varrho_{\mathrm{nv}}) &= \left(\frac{\varrho_{\mathrm{nv}}}{M_{\mathrm{nv}}} - \frac{\varrho_{\mathrm{tot}} - \varrho_{\mathrm{nv}}}{M_{\mathrm{H_2O}}}\right)^2 + \left({K^*}^2 + \frac{2K^*\varrho_{\mathrm{nv}}}{M_{\mathrm{nh}}} + \frac{2K^*(\varrho_{\mathrm{tot}} - \varrho_{\mathrm{nv}})}{M_{\mathrm{H_2O}}}\right). \end{aligned}$$

⋆

Remark 3.6 (Equations of state for concentrations and thermodynamic quantities)**.** In Example 3.5 we examplarily showed the reduction of the GENERIC structure under fast processes, which is based on the assumption that $\mathrm{T}_{\boldsymbol{C}}$ is invertible. Therefore, we can write the original concentrations $\boldsymbol{C}_i$ using an equation of state in terms of the new variable. Similarly, we can express all other derived thermodynamic quantities in terms of the new variables, e.g., chemical potential, temperature and pressure by

$$\tilde{\theta}(\tilde{\boldsymbol{q}}) = \theta(\mathrm{T}_{\boldsymbol{C}}^{-1}(\tilde{\boldsymbol{q}})), \quad \tilde{\boldsymbol{\mu}}(\tilde{\boldsymbol{q}}) = \boldsymbol{\mu}(\mathrm{T}_{\boldsymbol{C}}^{-1}(\tilde{\boldsymbol{q}})), \quad \tilde{\pi}_i(\tilde{\boldsymbol{q}}) = \pi_i(\mathrm{T}_{\boldsymbol{C}}^{-1}(\tilde{\boldsymbol{q}})), \quad \tilde{\boldsymbol{C}}_i(\tilde{\boldsymbol{q}}) = (\mathrm{T}_{\boldsymbol{C}}^{-1}(\tilde{\boldsymbol{q}}))_{\boldsymbol{C}_i}. \tag{3.21}$$

Remark 3.7 (The Gibbs energy minimization method)**.** The Gibbs energy minimization method is used for a wide variety of applications to multiphase/multicomponent systems [KP06], especially in geosciences where the size and heterogeneity of the system makes it disadvantageous to apply the direct approach described in Sec. 2.2. The main idea behind this method is to find the system composition for which its Gibbs energy is minimized, eventually subject to mass constraints. It can be shown by standard laws of thermodynamics [Con17] that a stable configuration corresponds to a minimum of the Gibbs energy. Although this idea could be applied to other free energies, the energy dependence on pressure π and temperature θ makes it particularly suited for geological applications. We focus here on the application of Gibbs energy minimization to chemical reactions and show that the equilibrium conditions met by this approach are (3.13). We consider the Gibbs energy related to a reactive system where reactions are described through a stoichiometric expression like (2.28) with N different components:

$$G^{\mathrm{sys}} := G^{\mathrm{sys}}(\pi, \theta, \boldsymbol{C}), \qquad \text{with } \boldsymbol{C} = (\boldsymbol{C}_i)_{i=1}^N. \tag{3.22}$$

We recall also that the Gibbs energy of a system can be obtained by means of a Legendre transform applied to the internal energy or Helmholtz free energy. Let us assume for the moment that only one reaction occurs. We define a new variable called *extent of reaction* $\xi : \Omega \to [0, 1]$ and write

$$\boldsymbol{C} = \boldsymbol{C}^0 + (\boldsymbol{\beta} - \boldsymbol{\alpha})\xi,$$

where $\boldsymbol{C}^0 = \boldsymbol{C}(t=0)$. We can rewrite (3.22) as a function of ξ:

$$G^{\mathrm{sys}} := G^{\mathrm{sys}}(\pi, \theta, \xi)\,, \tag{3.23}$$

then, by keeping pressure and temperature fixed and recalling that $\partial_{\boldsymbol{C}} G = \boldsymbol{\mu}$, the necessary condition for a minimum implies

$$\mathrm{D}_\xi G^{\mathrm{sys}}(\xi) = (\boldsymbol{\beta} - \boldsymbol{\alpha}) \cdot \boldsymbol{\mu} = 0\,, \tag{3.24}$$

which is again (3.13) for a single reaction.

4 Damped-Hamiltonian structure of models (1.1) and (1.2)

4.1 Limit of fast irreversible processes

In this section we reproduce the results from [PJP+17] in GENERIC form. The two-phase system introduced therein aims to model rock dehydration processes at their primal stage, that is when bounded water is released via chemical reactions and starts flowing through the newborn pore system. Although for the moment we will consider only one single reaction, other reactions are possibly involved in rock dehydration processes. Our example is the following dehydration reaction

$$(\mathrm{Mg,Fe})_{48}\mathrm{Si}_{34}\mathrm{O}_{85}(\mathrm{OH})_{62} + 20(\mathrm{Mg,Fe})(\mathrm{OH})_2 \rightleftharpoons 34(\mathrm{Mg,Fe})_2\mathrm{SiO}_4 + 51\mathrm{H}_2\mathrm{O}\,,$$

where antigorite $[(\mathrm{Mg,Fe})_{48}\mathrm{Si}_{34}\mathrm{O}_{85}(\mathrm{OH})_{62}]$ together with brucite $[(\mathrm{Mg,Fe})(\mathrm{OH}_2)]$ are transformed into olivine $[(\mathrm{Mg,Fe})_2\mathrm{SiO}_4]$ and a fluid phase $[\mathrm{H}_2\mathrm{O}]$. Antigorite is an abundant mineral in rocks that undergo subduction and is relevant in subduction zone dynamics because of its high water content. The reaction of antigorite and brucite to olivine and fluid is further discussed in Example 2.1 in a simplified version. We start from the full two-phase GENERIC system of the form

$$\dot{\boldsymbol{P}}_{\mathrm{s}} + \nabla \cdot (\boldsymbol{P}_{\mathrm{s}} \otimes \boldsymbol{v}_{\mathrm{s}}) = -\nabla \pi_{\mathrm{s}} - K_{\mathrm{D}} \boldsymbol{\gamma} + \nabla \cdot \boldsymbol{\sigma}_{\mathrm{s}}\,, \tag{4.1a}$$

$$\dot{\boldsymbol{P}}_{\mathrm{f}} + \nabla \cdot (\boldsymbol{P}_{\mathrm{f}} \otimes \boldsymbol{v}_{\mathrm{f}}) = -\nabla \pi_{\mathrm{f}} + K_{\mathrm{D}} \boldsymbol{\gamma} + \nabla \cdot \boldsymbol{\sigma}_{\mathrm{f}}\,, \tag{4.1b}$$

$$\dot{\boldsymbol{C}}_{\mathrm{s}} + \nabla \cdot (\boldsymbol{C}_{\mathrm{s}} \otimes \boldsymbol{v}_{\mathrm{s}}) = \sum_r k^r(\boldsymbol{q}) \left(\boldsymbol{C}^{\boldsymbol{\beta}^r} - \boldsymbol{C}^{\boldsymbol{\alpha}^r} \right) (\boldsymbol{\alpha}_{\mathrm{s}}^r - \boldsymbol{\beta}_{\mathrm{s}}^r)\,, \tag{4.1c}$$

$$\dot{\boldsymbol{C}}_{\mathrm{f}} + \nabla \cdot (\boldsymbol{C}_{\mathrm{f}} \otimes \boldsymbol{v}_{\mathrm{f}}) = \sum_r k^r(\boldsymbol{q}) \left(\boldsymbol{C}^{\boldsymbol{\beta}^r} - \boldsymbol{C}^{\boldsymbol{\alpha}^r} \right) (\boldsymbol{\alpha}_{\mathrm{f}}^r - \boldsymbol{\beta}_{\mathrm{f}}^r)\,, \tag{4.1d}$$

$$\dot{U}_{\mathrm{s}} + \nabla \cdot (U_{\mathrm{s}} \boldsymbol{v}_{\mathrm{s}}) = -\pi_{\mathrm{s}} \nabla \cdot \boldsymbol{v}_{\mathrm{s}} + \alpha K_{\mathrm{D}} |\boldsymbol{\gamma}|^2 + k_{\mathrm{he}} (\theta_{\mathrm{s}}^{-1} - \theta_{\mathrm{f}}^{-1}) + \nabla \cdot (k_{\mathrm{s}} \nabla \theta_{\mathrm{s}})\,, \tag{4.1e}$$

$$\dot{U}_{\mathrm{f}} + \nabla \cdot (U_{\mathrm{f}} \boldsymbol{v}_{\mathrm{f}}) = -\pi_{\mathrm{f}} \nabla \cdot \boldsymbol{v}_{\mathrm{f}} + (1-\alpha) K_{\mathrm{D}} |\boldsymbol{\gamma}|^2 - k_{\mathrm{he}} (\theta_{\mathrm{s}}^{-1} - \theta_{\mathrm{f}}^{-1}) + \nabla \cdot (k_{\mathrm{f}} \nabla \theta_{\mathrm{f}})\,, \tag{4.1f}$$

and assume that both heat-exchange and reactions are fast, i.e., $k_{\mathrm{he}}, k^r \to \infty$.

Fast thermal exchange Using fast heat-exchange we find new state variables with a combined internal energy $U = U_{\mathrm{s}} + U_{\mathrm{f}}$, following the evolution equation

$$\dot{U} + \nabla \cdot (U_{\mathrm{s}} \boldsymbol{v}_{\mathrm{s}} + U_{\mathrm{f}} \boldsymbol{v}_{\mathrm{f}}) = -\pi_{\mathrm{s}} \nabla \cdot \boldsymbol{v}_{\mathrm{s}} - \pi_{\mathrm{f}} \nabla \cdot \boldsymbol{v}_{\mathrm{f}} + K_{\mathrm{D}} |\boldsymbol{\gamma}|^2 + \nabla \cdot (k \nabla \theta) \tag{4.2}$$

where $k = k_\mathrm{s} + k_\mathrm{f}$. We can express $U_i = U_i(\boldsymbol{C}_\mathrm{s}, \boldsymbol{C}_\mathrm{f}, U)$ and all resulting thermodynamic quantities using the new state variable $\tilde{\boldsymbol{q}} = (\boldsymbol{P}_\mathrm{s}, \boldsymbol{C}_\mathrm{s}, \boldsymbol{P}_\mathrm{f}, \boldsymbol{C}_\mathrm{f}, U)$ under the assumption of $\theta_\mathrm{s} = \theta_\mathrm{f}$. As outlined in the previous section, this also produces an energy and entropy

$$\tilde{\mathcal{E}}(\tilde{\boldsymbol{q}}) = \int_\Omega \frac{\boldsymbol{P}_\mathrm{s}^2}{2\varrho_\mathrm{s}} + \frac{\boldsymbol{P}_\mathrm{f}^2}{2\varrho_\mathrm{f}} + U \,\mathrm{d}\boldsymbol{x}, \tag{4.3}$$

$$\tilde{\mathcal{S}}(\tilde{\boldsymbol{q}}) = \int_\Omega \tilde{S}(\boldsymbol{C}_\mathrm{s}, \boldsymbol{C}_\mathrm{f}, U) \,\mathrm{d}\boldsymbol{x}, \tag{4.4}$$

such that $\tilde{\mathcal{E}}(\tilde{\boldsymbol{q}}) = \mathcal{E}(\boldsymbol{q})$ and $\tilde{\mathcal{S}}(\tilde{\boldsymbol{q}}) = \mathcal{S}(\boldsymbol{q})$. This results in the new evolution $\dot{\tilde{\boldsymbol{q}}} = \tilde{\mathbb{J}}(\tilde{\boldsymbol{q}})\mathrm{D}\tilde{\mathcal{E}}(\tilde{\boldsymbol{q}}) + \tilde{\mathbb{K}}(\tilde{\boldsymbol{q}})\mathrm{D}\tilde{\mathcal{S}}(\tilde{\boldsymbol{q}})$. The previous Example 3.3 provides a practical recipe how the effective GENERIC dynamics is constructed.

Fast reactions In a similar spirit, we assume fast reactions and transform the fast reactions via $(\boldsymbol{C}_\mathrm{s}, \boldsymbol{C}_\mathrm{f})^\top \to Q(\boldsymbol{C}_\mathrm{s}, \boldsymbol{C}_\mathrm{f})^\top$, where the column vectors of $Q^\top$ span the space $\Gamma^\perp$ orthogonal to the stoichiometric space Γ defined in (3.17). Since $\boldsymbol{M} \in \Lambda^\perp$ we will always use the conservation of total mass (2.21) as one evolution equation. As suggested in [PJP+17], we also assume that the dehydration processes can be formulated in terms of the mass density of non-volatile solids $\varrho_\mathrm{nv} = \varrho_\mathrm{s}(1 - X_h)$, which can be obtained through the transformation Q. Here, $0 \le X_h \le 1$ is the relative hydrous content of the solid (rock) phase, that can potentially converted into the fluid phase. The precise definition of X_h depends on the interpretation of the components in $\boldsymbol{M} = (\boldsymbol{M}_\mathrm{s}, \boldsymbol{M}_\mathrm{f})^\top$. Having the invertibility of the corresponding equilibrium constraints from the Gibbs minimization we can write $\boldsymbol{C}_i = \boldsymbol{C}_i(\tilde{\boldsymbol{q}})$ and all remaining thermodynamic quantities with the help of the reduced concentration-like variables $\boldsymbol{C}^\perp = (\varrho, \varrho_\mathrm{nv}, ...) = Q\boldsymbol{C}$ assuming that the reactions are in equilibrium. As before, we can define the driving energy $\tilde{\mathcal{E}}(\tilde{\boldsymbol{q}})$ and entropy $\tilde{\mathcal{S}}(\tilde{\boldsymbol{q}})$ for this evolution in terms of the new state variable $\tilde{\boldsymbol{q}} = (\boldsymbol{P}_\mathrm{s}, \boldsymbol{P}_\mathrm{f}, U, \boldsymbol{C}^\perp)$. While details of this construction depend on the stoichiometry and the original entropy density, the final result maintains the GENERIC structure with modified operators and driving functionals. A concrete example relating to fast dehydration reactions as in (4.1) was provided in Example 3.5.

4.2 Discussion of model (1.1)

We assume that by the limit of fast irreversible processes for heat exchange and reactions we have obtained a GENERIC formulation for $\boldsymbol{q} = (\boldsymbol{P}_\mathrm{s}, \boldsymbol{P}_\mathrm{f}, U, \boldsymbol{C}^\perp)^\top$ with driving energy $\tilde{\mathcal{E}}(\tilde{\boldsymbol{q}})$ and entropy $\tilde{\mathcal{S}}(\tilde{\boldsymbol{q}})$ as they were constructed before. In geoscientific applications, however, evolution equations are usually formulated in certain compositional variables [PJP+17, BJV+20, HVJ22], which we address below.

For simplicity, we assume that the reduced concentrations are $\boldsymbol{C}^\perp = (\varrho_\mathrm{tot}, \varrho_\mathrm{nv})$, i.e., the total mass density and the mass density of non-volatile solids. For more complex systems and other slow processes one might have to include further state variables into $\boldsymbol{C}^\perp$.

For each phase $i \in \{\mathrm{s}, \mathrm{f}\}$ we assume the existence of *volume fractions* $\phi_i : \Omega \to [0, 1]$, such that

$$0 \le \phi_i(\boldsymbol{x}) \le 1 \qquad \text{for all } \boldsymbol{x} \in \Omega \text{ and} \tag{4.5a}$$

$$\phi_\mathrm{s}(\boldsymbol{x}) + \phi_\mathrm{f}(\boldsymbol{x}) = 1 \qquad \text{for all } \boldsymbol{x} \in \Omega\,. \tag{4.5b}$$

Based on these variables it is now possible to define "pure" mass densities, i.e., the value of ϱ_i if only phase i would be present in the system,

$$\hat{\varrho}_\mathrm{i} := \frac{\varrho_i}{\phi_i}\,, \qquad \text{for } i \in \{\mathrm{s}, \mathrm{f}\}\,. \tag{4.6}$$

Similarly, it is possible to generalize the previous relation for any extensive variable A^i and distinguish it between "pure" and "partial" where the former will be denoted by $\hat{A}^i$ and related via

$$A^i(\boldsymbol{x}) = \hat{A}^i(\boldsymbol{x})\phi_i(\boldsymbol{x})\,, \qquad \text{for } i \in \{\mathrm{s},\mathrm{f}\}\,.$$

Remark 1 (Weight fractions)**.** Another commonly used variable is the weight fraction X_h of a given chemical compound h, where h could be a species C_i itself or just part of it. Here we are interested in the weight fraction of bound water within the solid phase. We will denote it by $X_{b\mathrm{H_2O}}$ and introduce

$$\varrho_{\mathrm{s}}(1 - X_{b\mathrm{H_2O}}) = \varrho_{\mathrm{nv}} \quad \Leftrightarrow \quad \hat{\varrho}_{\mathrm{s}}(1 - X_{b\mathrm{H_2O}}) = \hat{\varrho}_{\mathrm{nv}} \tag{4.7}$$

for the system described above.

In total this gives the following evolution equations for the two-phase system

$$\partial_t \boldsymbol{P}_{\mathrm{s}} = -\nabla\cdot(\boldsymbol{P}_{\mathrm{s}}\otimes\boldsymbol{v}_{\mathrm{s}}) - \nabla\pi_{\mathrm{s}} + K_{\mathrm{D}}\left(\boldsymbol{v}_{\mathrm{f}} - \boldsymbol{v}_{\mathrm{s}}\right)\,, \tag{4.8a}$$

$$\partial_t \boldsymbol{P}_{\mathrm{f}} = -\nabla\cdot(\boldsymbol{P}_{\mathrm{f}}\otimes\boldsymbol{v}_{\mathrm{f}}) - \nabla\pi_{\mathrm{f}} - K_{\mathrm{D}}\left(\boldsymbol{v}_{\mathrm{f}} - \boldsymbol{v}_{\mathrm{s}}\right)\,, \tag{4.8b}$$

$$\dot{U} + \nabla\cdot(U_{\mathrm{s}}\boldsymbol{v}_{\mathrm{s}} + U_{\mathrm{f}}\boldsymbol{v}_{\mathrm{f}}) = -\pi_{\mathrm{s}}\nabla\cdot\boldsymbol{v}_{\mathrm{s}} - \pi_{\mathrm{f}}\nabla\cdot\boldsymbol{v}_{\mathrm{f}} + K_{\mathrm{D}}\left|\boldsymbol{v}_{\mathrm{f}} - \boldsymbol{v}_{\mathrm{s}}\right|^2 + \nabla\cdot(k\nabla\theta)\,, \tag{4.8c}$$

$$\partial_t \varrho_{\mathrm{tot}} \equiv \partial_t\big((1-\phi_{\mathrm{f}})\hat{\varrho}_{\mathrm{s}} + \phi_{\mathrm{f}}\hat{\varrho}_{\mathrm{f}}\big) = -\nabla\cdot\left((1-\phi_{\mathrm{f}})\hat{\varrho}_{\mathrm{s}}\boldsymbol{v}_{\mathrm{s}} + \phi_{\mathrm{f}}\hat{\varrho}_{\mathrm{f}}\boldsymbol{v}_{\mathrm{f}}\right), \tag{4.8d}$$

$$\partial_t \varrho_{\mathrm{nv}} \equiv \partial_t((1-\phi_{\mathrm{f}})\hat{\varrho}_{\mathrm{nv}}) = -\nabla\cdot\left((1-\phi_{\mathrm{s}})\hat{\varrho}_{\mathrm{nv}}\boldsymbol{v}_{\mathrm{s}} + Q_{\mathrm{nv,k}}\,\boldsymbol{j}_k\right), \tag{4.8e}$$

where at this point the evolution for the volume fraction ϕ is not yet determined. For a discussion of this evolution we refer to [MR13, Ehl09]. However, we will assume that the solid is immobile, i.e., $\boldsymbol{v}_{\mathrm{s}} = 0$ such that

$$\phi_{\mathrm{f}}(t) = 1 - \frac{(1-\phi_{\mathrm{f}}(t=0))\hat{\varrho}_{\mathrm{nv}}(t=0)}{\hat{\varrho}_{\mathrm{nv}}(t)}, \tag{4.9}$$

e.g. see [PJP$^+$17, Eq. 11]. In this equation, as discussed in Example 3.5, $\hat{\varrho}_{\mathrm{s}}$, $\hat{\varrho}_{\mathrm{f}}$ are given by an equation of state as in (3.21) and the weight fraction for water is given by (4.7).

Neglecting the diffusion flux in the non-volatile solid and making the identification of the Darcy flux $\boldsymbol{v}_{\mathrm{f}} = -K_{\mathrm{D}}^{-1}\nabla\pi_{\mathrm{f}}$, setting the temperature to a given constant, the evolution equations for the mass densities become

$$\partial_t\left(\hat{\varrho}_{\mathrm{s}}(1 - X_{b\mathrm{H_2O}})(1-\phi_{\mathrm{f}})\right) = 0\,, \tag{4.10a}$$

$$\partial_t\left(\hat{\varrho}_{\mathrm{s}}(1-\phi_{\mathrm{f}}) + \hat{\varrho}_{\mathrm{l}}\phi_{\mathrm{f}}\right) = \nabla\cdot\left(\frac{\phi_{\mathrm{f}}\hat{\varrho}_{\mathrm{f}}}{K_{\mathrm{D}}}\nabla\pi_{\mathrm{f}}\right)\,. \tag{4.10b}$$

This is, in fact, an evolution system for the unknowns ϱ_{nv} and ϱ_{tot}. However, the construction in [PJP$^+$17] suggests that a change of variables in the sense of [ZPT21] should be applied, where the equations of state are determined as functions of temperature θ and fluid pressure π_{f}. This is the model (1.1) from [PJP$^+$17].

4.3 Discussion of model (1.2)

Analogously to what is described in Sec. 4.2 we can obtain system (1.2) as a GENERIC system in the limit of fast irreversible processes for temperature and reactions equilibration. In this case we will also account for

reactions in which other species are released along with the fluid and are subject to diffusion. An example for this type of reaction is:

$$(\mathrm{Mg,Fe})_{48}\mathrm{Si}_{34}\mathrm{O}_{85}(\mathrm{OH})_{62} \rightleftharpoons 34(\mathrm{Mg,Fe})_2\mathrm{SiO}_4 + 31\mathrm{H}_2\mathrm{O} + 10{\mathrm{SiO}_2}^{\mathrm{aq}}\,,$$

where ${\mathrm{SiO}_2}^{\mathrm{aq}}$ on the product-side (right) diffuses within the fluid. Therefore we extend the GENERIC system (4.1) by adding the diffusive Onsager operator (2.26). Herein, since no solid-state diffusion is assumed here, we set all diffusion coefficients except for that of $C_{\mathrm{f},\mathrm{SiO}_2}$ to zero. System (1.2) is then recovered taking the limits of fast heat exchange and of fast reactions, for which we assume the reduced concentration vector to be $\boldsymbol{C}^{\perp} = (\varrho_{\mathrm{tot}}, \varrho_{\mathrm{nv}}, \varrho_{\mathrm{SiO}_2})$. By assuming zero solid velocity, i.e., $\boldsymbol{v}_{\mathrm{s}} = \boldsymbol{0}$ and conservation of the non-volatile mass density ϱ_{nv}, the evolution equations of $\boldsymbol{C}^{\perp}$ give exactly (1.2a)-(1.2c). Furthermore, it should be noted that in applications a variable is often used to denoted the total amount of a particular chemical element or constituent in a compound/phase. In this way, the content of k-th component in the i-th phase can be defined as follows

$$c_{\mathrm{i}}^{k} := \frac{M_{\mathrm{i},k} C_{\mathrm{i},k}}{\varrho_{\mathrm{i}}}\,.$$

In equations (1.2) we omit the superscript SiO_2 since no misunderstanding is possible. In fact, (1.2b) is the evolution equation for $\varrho_{\mathrm{SiO}_2} = \varrho_{\mathrm{s}} c_{\mathrm{s}}(1-\phi) + \varrho_{\mathrm{f}} c_{\mathrm{f}} \phi$.

4.4 Geological interpretation of the models

The model defined by the set of equations (4.10), resp. (1.1), describes the general case of fluid flow through a porous rock where mass is exchanged between the fluid and the solid phase by mineral dissolution and precipitation. The assumption of an immobile solid, i.e., of zero solid velocity, is valid for small length scales (sub-m to mm) where gravitational effects can be neglected because the density contrast is small compared to the variations in fluid pressure controlled by the local thermodynamic equilibrium.

On such small length scales the large-scale temperature gradients, see Fig. 1, can be neglected and thus, for a given pressure and temperature, the local bulk composition controls when the dehydration reaction occurs. Therefore, chemical heterogeneities, i.e., local bulk composition variations in the domain, and chemical processes such as reactive fluid flow dominate rock dehydration on small length scales. Such variations in the composition are taken into account in model (1.2) in terms of the silicon dioxide SiO_2 content c_{s} and its diffusion and transport.

The focus of this study on the dehydration reaction of antigorite and brucite sets certain limits to the range of variables of models (1.1) and (1.2), especially the values for temperature, pressure and c_{s}. Pressure and temperature are confined to values that occur during ongoing subduction and c_{s} is limited to values where the minerals of interest are stable.

As antigorite and brucite form solid solutions between magnesium (Mg)- and iron (Fe)-endmembers, the reaction occurs not at a single point in π-θ space but rather in a divariant π-θ field. The onset of the reaction typically occurs at around 350 °C with the reaction of Fe-rich antigorite and brucite and is limited to higher temperatures by the stability limit of Mg-rich brucite at around 550 °C. Pressures depend on the depth at which the slab reaches those temperatures and on the fluid pressure that is controlled by the local thermodynamic equilibrium of the reaction. Typical lithostatic pressures, i.e. the pressure exerted on the solid by the overlying rock column, are in the range of 1-2.5 GPa (for a compilation of π-θ paths during subduction see e.g. [SvKA10]).

The third variable controlling the stable mineral assemblage is the rock composition. A serpentinite that consists entirely of antigorite has a bulk Si content of $c_{\mathrm{s}} \approx 0.205$. However, Si is distributed heterogeneously in the rock

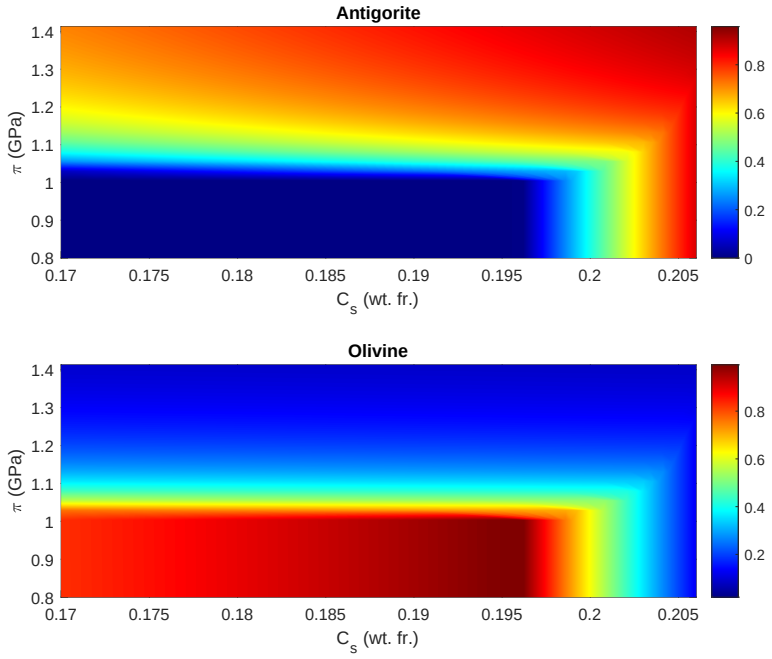

Figure 3: Abundances (volume fraction) of antigorite (hydrated mineral) and olivine (dehydrated mineral) as a function of silica content in the solid (c_s) and pressure (π) for a fixed temperature θ = 480 °C. An almost olivine-pure mineral assemblage forms at $c_s \approx 0.19$ for pressures below 1 GPa while for higher values antigorite becomes the dominant phase. Again, we underline that these plots are for a given composition at a given temperature, however the qualitative behaviour does not change for composition and temperature within the range of values discussed in Section 4.4.

and c_{s} can therefore vary on smaller local domains within the rock. At low temperatures, c_{s} values below 0.205 lead to an increase of brucite abundance. A domain with a Si content of $c_{\mathrm{s}} \approx 0.17$ contains significant amounts of brucite and antigorite at lower temperatures. At higher temperatures, this domain will form an almost pure olivine mineral assemblage. We therefore limit the range of c_s values to $0.17 - 0.205$ because in this range the mineral assemblage consists of various proportions of antigorite, olivine and brucite. For values $c_{\mathrm{s}} > 0.205$ talc, another hydrous mineral that dehydrates to the dry mineral orthopyroxene, becomes stable. This dehydration reaction however is not within the scope of this study.

5 Towards the analysis of models (1.1) and (1.2)

In this section we discuss first steps and results on the mathematical analysis of models (1.1) and (1.2). Our approach combines a Galerkin approximation in space with an implicit Euler scheme in time as to provide a convergence result for a discretization scheme close to that already used in [PJP+17, HVJ22] for their numerical implementation. As a first step, we revisit the two models and reformulate them as a system of parabolic equations by means of a suitable transformation of variables. Based on this we state first existence results, which are deduced in detail in [ZT23]. Our mathematical results require certain smoothness assumptions for the transformation maps and the resulting coefficient functions. We validate them in detail for specific thermodynamical rock data in Sections 5.1.3 and 5.2.3. This perusal will show that the mathematical assumptions are

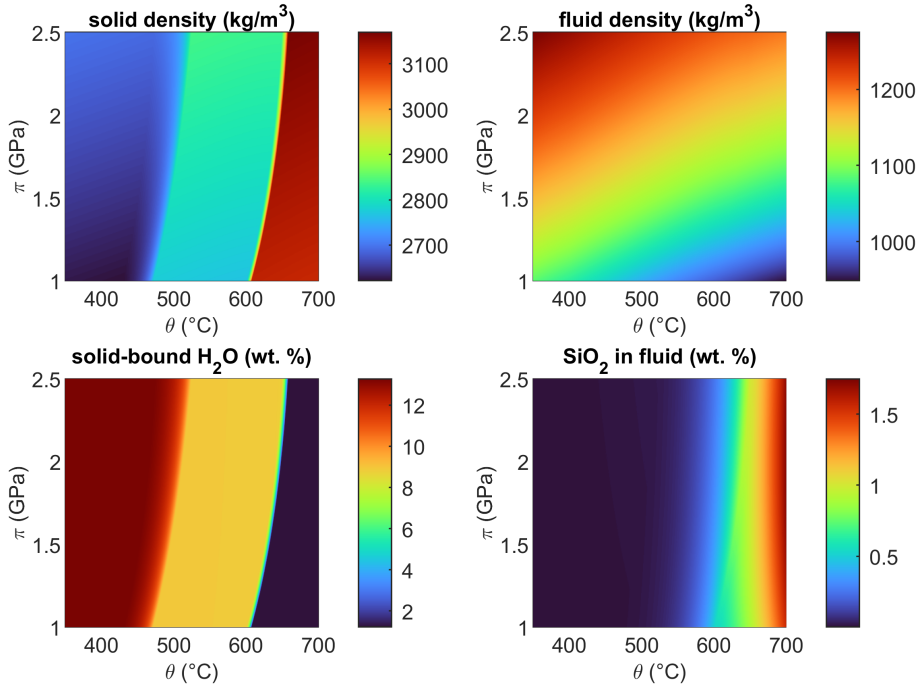

Figure 4: Pressure-temperature dependence of solid density, fluid density, solid-bound H_2O content and fluid composition wrt. SiO_2 for a typical serpentinite bulk rock composition as also used in the model of [HVJ22]. Their model uses these pre-computed values as lookup tables to close the system of equations. One can see the qualitative changes of these functions for different values of (π, θ). More specifically, the rapid change in color for the solid mass density in the top left corner at fixed θ with varying π corresponds to a kink w.r.t. π of the type shown in Fig. 5.

met in a certain "good"range of the thermodynamical data set but violated in another regime of the data set. We prove that a well-prepared initial datum keeps a solution within the good range for all times.

In this section we will denote the “pure” mass densities by ϱ_{s} and ϱ_{f} in contrast to $\hat{\varrho}_{\mathrm{s}}$ and $\hat{\varrho}_{\mathrm{f}}$ in model (1.1) and (1.2).

5.1 Results and challenges of model (1.1)

5.1.1 Parabolic form of system (1.1)

Model (1.1) consists of the conservation of the mass of non-volatile species (1.1a) and of the conservation of total mass (1.1b). As a direct consequence of relation (1.1a) the porosity ϕ can be explicitly determined as follows

$$\phi = 1 - \frac{\varrho_{\mathrm{s}}^0(1-X_{\mathrm{h}}^0)(1-\phi^0)}{\varrho_{\mathrm{s}}(1-X_{\mathrm{h}})}\,. \tag{5.1}$$

It is further assumed in [PJP+17] for the mass densities ϱ_{s} and ϱ_{f} of the solid and the fluid, and for the fraction X_{h} of fluid stored in the solid that

$$\begin{aligned}&\varrho_{\mathrm{s}} = \tilde{\varrho}_{\mathrm{s}}(\pi,\theta), \quad \varrho_{\mathrm{f}} = \tilde{\varrho}_{\mathrm{f}}(\pi,\theta), \quad \text{and } X_{\mathrm{h}} = \tilde{X}_{\mathrm{h}}(\pi,\theta)\\ &\text{are functions of pressure } \pi \text{ and temperature } \theta.\end{aligned} \tag{5.2}$$

Although the closed mathematical expression for these functions is not known, the values of $\varrho_{\mathrm{s}}, \varrho_{\mathrm{f}}, X_{\mathrm{h}}$ in dependence of π and θ can be recovered from thermodynamical data tables. An example of data so produced is shown in Fig. 4. Due to this, also the porosity can be seen as a function of π and θ, while also dependent on the initial data $\varrho_{\mathrm{s}}^0, X_{\mathrm{h}}^0$ as well , i.e. (5.1) gives

$$\phi = 1 - \tfrac{\varrho_{\mathrm{s}}^0(1-X_{\mathrm{h}}^0)(1-\phi^0)}{\tilde{\varrho}_{\mathrm{s}}(\pi,\theta)(1-\tilde{X}_{\mathrm{h}}(\pi,\theta))} =: \tilde{\phi}(\pi,\theta)\,. \tag{5.3}$$

Similarly, the terms appearing in (1.1b) can be rewritten as functions of π and θ, i.e., we introduce

$$\tilde{\varrho}(\pi,\theta) := (\tilde{\varrho}_{\mathrm{f}}(\pi,\theta)\tilde{\phi}(\pi,\theta) + \tilde{\varrho}_{\mathrm{s}}(\pi,\theta)(1-\tilde{\phi}(\pi,\theta))) \quad \text{and} \tag{5.4}$$

$$\widetilde{\mathrm{K}}(\pi,\theta) := \tilde{\varrho}_{\mathrm{f}}(\pi,\theta)K_\phi(\tilde{\phi}(\pi,\theta)) = \tilde{\varrho}_{\mathrm{f}}(\pi,\theta)\tfrac{\kappa}{\mu}\tilde{\phi}(\pi,\theta)^3 \text{ with constants } \kappa,\mu>0 \tag{5.5}$$

for the total mass and for the permeability. Then (1.1b) takes the form

$$\partial_t\tilde{\varrho}(\pi,\theta) = \nabla\cdot\widetilde{\mathrm{K}}(\pi,\theta)\nabla\pi\,. \tag{5.6}$$

Now we set

$$\varrho := \tilde{\varrho}(\pi,\theta) \tag{5.7}$$

and we assume that

$$\text{for all } \theta>0 \text{ fixed the function } \tilde{\varrho}(\cdot,\theta) \text{ is invertible in } \pi, \tag{5.8a}$$

$$\text{the inverse function } \tilde{\varrho}^{-1}(\cdot,\theta) \text{ is continuously differentiable, and} \tag{5.8b}$$

$$\text{there are constants } 0<c_*<c^* \text{ such that } \tfrac{1}{c^*} < \partial_\varrho\tilde{\varrho}^{-1}(\varrho,\theta) = \frac{1}{\partial_\pi\tilde{\varrho}(\tilde{\varrho}^{-1}(\tilde{\varrho}(\pi,\theta),\theta),\theta)} < \tfrac{1}{c_*}\,. \tag{5.8c}$$

Thus, for any $\theta>0$ fixed we find

$$\pi = \tilde{\pi}(\varrho,\theta) := \tilde{\varrho}^{-1}(\varrho,\theta)\,. \tag{5.9}$$

Due to the fast equilibration of temperature discussed for the model (1.1) in Sec. 4, we can assume that θ is constant in space. Thus, in view of (5.8) together with the chain rule and the rule for differentiating the inverse we calculate

$$\nabla\pi = \nabla\tilde{\pi}(\varrho,\theta) = \partial_\varrho\tilde{\pi}(\varrho,\theta)\nabla\varrho = \frac{1}{\partial_\pi\tilde{\varrho}(\tilde{\pi}(\varrho,\theta),\theta)}\nabla\varrho \tag{5.10}$$

This gives the relation

$$\widetilde{\mathrm{K}}(\pi,\theta)\nabla\pi = \widehat{\mathrm{K}}(\varrho,\theta)\nabla\varrho \text{ with } \widehat{\mathrm{K}}(\varrho,\theta) = \frac{\widetilde{\mathrm{K}}(\tilde{\pi}(\varrho,\theta),\theta)}{\partial_\pi\tilde{\varrho}(\tilde{\pi}(\varrho,\theta),\theta)}\,. \tag{5.11}$$

Hence, (5.6) can be rewritten as a parabolic equation for the total mass density ϱ

$$\partial_t\varrho = \nabla\cdot\widehat{\mathrm{K}}(\varrho,\theta)\nabla\varrho\,. \tag{5.12}$$

Furthermore, for $\widehat{\mathrm{K}}$ we make the assumptions

$$\text{for all } \theta>0 \text{ fixed the function } \widehat{\mathrm{K}}(\varrho,\theta) \text{ is continuous and} \tag{5.13a}$$

$$\text{there are constants } 0<\hat{k}_*<\hat{k}^* \text{ such that } \hat{k}_* \le \widehat{\mathrm{K}}(\varrho,\theta) \le \hat{k}^* \text{ for all } \varrho\in\mathbb{R}. \tag{5.13b}$$

We point out that above assumptions (5.13) are satisfied if $\widetilde{\mathrm{K}}$ is continuous and uniformly bounded, and if properties (5.8) hold true. This, in turn, is closely linked to the properties of the given functions $\tilde{\phi}(\cdot,\theta)$, $\tilde{\varrho}_{\mathrm{s}}(\cdot,\theta)$, $\tilde{\varrho}_{\mathrm{f}}(\cdot,\theta)$, and $\tilde{X}_{\mathrm{h}}$.

5.1.2 Existence of a weak solution

Thanks to the above assumptions (5.13) one can deduce the existence of a weak solution $\varrho : [0,T] \times \Omega \to (0,\infty)$ for the transformed system (5.12). Since the assumptions (5.8) guarantee the bijectivity of the transformation map one can also infer the existence of a weak solution $\pi : [0,T] \times \Omega \to (0,\infty)$ for the original system (1.1). Our existence result reads as follows:

Theorem 5.1 (Existence of a weak solution for system (5.12))**.** *Let $\mathsf{T} > 0$ and let $\Omega \subset \mathbb{R}^d$ be a bounded Lipschitz domain. Let $Q_{\mathsf{T}} := (0,\mathsf{T}) \times \Omega$ denote the space-time cylinder and set*

$$V := H^1(\Omega)\,. \tag{5.14}$$

Then the following statements hold true:

1 *Let $\varrho_0 \in V$ be a given initial datum and assume that $\widehat{\mathrm{K}}(\cdot,\theta)$ satisfies* (5.13)*. Then there exists a function*

$$\varrho \in H^1(0,\mathsf{T};V^*) \cap L^2(0,\mathsf{T};V) \cap L^\infty(0,\mathsf{T};L^2(\Omega)) \cap C^0([0,\mathsf{T}];L^2(\Omega))\,, \tag{5.15a}$$

which satisfies

$$\int_{Q_{\mathsf{T}}} \Big(\partial_t \varrho v + \widehat{\mathrm{K}}(\varrho,\theta)\nabla\varrho\cdot\nabla v \Big)\,\mathrm{d}x\,\mathrm{d}t = 0 \quad \textit{for all } v \in L^2(0,\mathsf{T};V) \tag{5.15b}$$

and $\varrho(0) = \varrho_0$.

2 *Further assume that there are constants $0 < r_* < r^*$ such that $r_* \le \varrho_0(x) \le r^*$ holds true for a.e. $x \in \Omega$ for the initial datum ϱ_0. Then for all $t \in [0,\mathsf{T}]$ also a solution ϱ satisfies $r_* \le \varrho(t,x) \le r^*$ for a.e. $x \in \Omega$.*

Comments on the proof: We refer to [ZT23, Sec. 3, 4] for the details of the proof. Here we give a short outline of the main steps.

To 1. In order to prove the existence of a weak solution satisfying (5.15) we introduce a discretization in time $\mathbb{T}_\tau := \{t_\tau^0 = 0,\, t_\tau^k = k\tau \text{ for } \tau = \mathsf{T}/N,\, k = 1,\dots,N \in \mathbb{N}\}$ and a Galerkin approximation in space by finite-dimensional subspaces $V^n = \operatorname{span}\{e_1,\dots,e_n\} \subset V$, $n \in \mathbb{N}$ such that $\bigcup_{n\in\mathbb{N}} V^n \subset V$ densely, with e_i, $i = 1,\dots,n$ denoting a basis of V^n . By invoking [Zei86, Prop. 2.8, p. 53] we obtain for every time-step $k \le N$, all $N \in \mathbb{N}$, and all $n \in \mathbb{N}$ the existence of a vector of coefficients $\vec{\varrho}_n^{\tau k} = (\varrho_{n1}^{\tau k},\dots,\varrho_{nn}^{\tau k})$ providing an element $\varrho_n^{\tau k} = \sum_{i=1}^n \varrho_{ni}^{\tau k} e_i \in V^n$ that solves the system of n nonlinear equations

$$\sum_{i=1}^n \int_\Omega \Big(\frac{\varrho_{ni}^{\tau k} - \varrho_{ni}^{\tau k-1}}{\tau} e_i e_j + \widehat{\mathrm{K}}(\varrho_n^{\tau k},\theta)\varrho_{ni}^{\tau k}\nabla e_i\cdot\nabla e_j \Big)\,\mathrm{d}x = 0 \quad \text{for all } j = 1,\dots,n. \tag{5.16}$$

By testing (5.16) with $\varrho_n^{\tau k} \in V^n$ and summing up over $k \le l \in \{1,\dots,N\}$ one obtains the following a priori estimates uniformly for all $n \in \mathbb{N}$ and $\tau = \mathsf{T}/N$, $N \in \mathbb{N}$:

$$\tfrac{1}{2}\|\varrho_n^{\tau l}\|_{L^2(\Omega)}^2 + \sum_{k=1}^l \tau\hat{k}_*\|\nabla\varrho_n^{\tau k}\|_{L^2(\Omega,\mathbb{R}^d)}^2 \le \tfrac{1}{2}\|\varrho_n^{\tau 0}\|_{L^2(\Omega)}^2 = \|\mathbb{P}_n\varrho_0\|_{L^2(\Omega)}^2\,, \qquad \text{hence:}$$

$$\tfrac{1}{2}\|\varrho_n^{\tau l}\|_{L^2(\Omega)}^2 + \sum_{k=1}^l \tau\hat{k}_*\|\varrho_n^{\tau k}\|_V^2 \le (\tfrac{1}{2} + \mathsf{T}\hat{k}_*)\|\mathbb{P}_n\varrho_0\|_{L^2(\Omega)}^2\,, \tag{5.17}$$

where $\mathbb{P}_n \varrho_0$ is the projection of the initial datum $\varrho_0 \in V$ into V^n and where we have also used (5.13). For each $k \in \{1, \dots, N\}$, with $N \in \mathbb{N}$ fixed, as $n \to \infty$, this provides the existence of a (not relabelled) subsequence $(\varrho_n^{\tau k})_{n\in\mathbb{N}}$ and of an element $\varrho^{\tau k} \in V$ such that

$$\varrho_n^{\tau k} \rightharpoonup \varrho^{\tau k} \quad \text{in } V \quad \text{as } n \to \infty\,. \tag{5.18}$$

By the compact embedding $V \Subset L^2(\Omega)$ and the boundedness of $\widehat{\mathrm{K}}$ we conclude by the dominated convergence theorem that $\widehat{\mathrm{K}}(\varrho_n^{\tau k})\nabla \mathbb{P}_n v \to \widehat{\mathrm{K}}(\varrho_n^{\tau k})\nabla v$ for every test function $v \in V$ and for all $k \in \{1, \dots, N\}$, and $\tau = \mathsf{T}/N$, $N \in \mathbb{N}$. Therefore we deduce by weak-strong convergence arguments that

$$0 \;=\; \sum_{k=1}^{N} \tau \int_\Omega \Big(\frac{\varrho_n^{\tau k} - \varrho_n^{\tau k-1}}{\tau} \mathbb{P}_n v^{\tau k} + \widehat{\mathrm{K}}(\varrho_n^{\tau k}, \theta) \nabla \varrho_n^{\tau k} \cdot \nabla \mathbb{P}_n v^{\tau k} \Big)\, \mathrm{d}x \tag{5.19a}$$

$$\downarrow\; n \to \infty$$

$$0 \;=\; \sum_{k=1}^{N} \tau \int_\Omega \Big(\frac{\varrho^{\tau k} - \varrho^{\tau k-1}}{\tau} v^{\tau k} + \widehat{\mathrm{K}}(\varrho^{\tau k}, \theta) \nabla \varrho^{\tau k} \cdot \nabla v^{\tau k} \Big)\, \mathrm{d}x \quad \text{for all } v^{\tau k} \in V. \tag{5.19b}$$

We introduce the piecewise constant $\overline{\varrho}_\tau$, $\underline{\varrho}_\tau$, and affine ϱ_τ interpolants in time, i.e., for any $t \in (t_\tau^{k-1}, t_\tau^k]$, $k = 1, \dots, N$ we set

$$\overline{\varrho}_\tau(t) := \varrho^{\tau k},\ \underline{\varrho}_\tau(t) := \varrho^{\tau k-1},\ \varrho_\tau(t) := \frac{t - t_\tau^{k-1}}{\tau} \varrho^{\tau k} + \frac{t_\tau^k - t}{\tau} \varrho^{\tau k-1} \quad \text{as well as } \bar{t}_\tau(t) := t_\tau^k\,, \tag{5.20}$$

and we write $\dot{\varrho}_\tau(t) = (\varrho^{\tau k} - \varrho^{\tau k-1})/\tau$, $k \in \{1, \dots, N\}$, for the time-derivative of the affine interpolant ϱ_τ. We approximate any test function $v \in L^2(0, \mathsf{T}; V)$ by

$$v^{\tau k} := \frac{1}{\tau} \int_{t_\tau^{k-1}}^{t_\tau^k} v(s)\, \mathrm{d}s$$

and use these values to introduce the interpolants $\overline{v}_\tau$, $\underline{v}_\tau$, and v_τ as in (5.20). This ensures strong convergence of the interpolants, i.e., $\overline{v}_\tau, \underline{v}_\tau, v_\tau \to v$ strongly in $L^2(0, \mathsf{T}; V)$. Moreover, for the interpolants $(\overline{\varrho}_\tau, \underline{\varrho}_\tau, \varrho_\tau)$ the estimate (5.17) together with (5.19) provides the following bounds uniformly in $\tau = \mathsf{T}/N$, $N \in \mathbb{N}$:

$$\|\overline{\varrho}_\tau\|_{\mathrm{B}(0,\mathsf{T};L^2(\Omega))} + \|\underline{\varrho}_\tau\|_{\mathrm{B}(0,\mathsf{T};L^2(\Omega))} + \|\varrho_\tau\|_{\mathrm{B}(0,\mathsf{T};L^2(\Omega))} \;\leq\; C\,, \tag{5.21a}$$

$$\|\overline{\varrho}_\tau\|_{L^2(0,\mathsf{T};V)} \;\leq\; C\,, \tag{5.21b}$$

$$\|\dot{\varrho}_\tau\|_{L^2(0,\mathsf{T};V^*)} \;\leq\; C\,, \tag{5.21c}$$

with a constant $C > 0$ independent of $\tau = \mathsf{T}/N$ and $N \in \mathbb{N}$. Accordingly, one concludes the existence of a (not relabelled) subsequence and of a limit ϱ of regularity (5.15a) such that the following convergence properties hold true:

$$\overline{\varrho}_\tau, \underline{\varrho}_\tau, \varrho_\tau \;\overset{*}{\rightharpoonup}\; \varrho \quad \text{weakly-}* \text{ in } L^\infty(0, \mathsf{T}; L^2(\Omega))\,, \tag{5.22a}$$

$$\overline{\varrho}_\tau, \varrho_\tau \;\rightharpoonup\; \varrho \quad \text{weakly in } L^2(0, \mathsf{T}; V)\,, \tag{5.22b}$$

$$\dot{\varrho}_\tau \;\rightharpoonup\; \dot{\varrho} \quad \text{weakly in } L^2(0, \mathsf{T}; V^*)\,, \tag{5.22c}$$

$$\overline{\varrho}_\tau, \varrho_\tau \;\to\; \varrho \quad \text{strongly in } L^2(0, \mathsf{T}; L^2(\Omega))\,, \tag{5.22d}$$

$$\overline{\varrho}_\tau(t), \underline{\varrho}_\tau(t), \varrho_\tau(t) \;\overset{*}{\rightharpoonup}\; \varrho(t) \quad \text{weakly-}* \text{ in } V^* \text{ for all } t \in [0, \mathsf{T}]\,. \tag{5.22e}$$

Here, convergences (5.22a)-(5.22c) follow from standard compactness arguments. Moreover, convergence (5.22d) is deduced from estimates (5.21b) and (5.21c) by means of a time-discrete version of the Aubin-Lions

lemma, cf. [DJ12, Thm. 1]. We further observe that estimates (5.21a) and (5.21c) result in a uniform bound for the interpolants in $BV(0,\mathsf{T};V^*)$. From this, the pointwise convergence in time (5.22e) ensues by means of Helly's selection principle [MR15, Thm. B.5.10, p. 610]. Convergence results (5.22) then enable us to pass to the limit in $\tau = \mathsf{T}/N \to 0$ as $N \to \infty$ in (5.19b) and to conclude the validity of the weak formulation (5.15b). In addition, convergence result (5.22e) allows it to deduce that the initial datum is attained, i.e. that $\varrho(0) = \varrho_0$ in V. Let us also note that the regularity $\varrho \in H^1(0,\mathsf{T};V^*) \cap L^2(0,\mathsf{T};V) \cap L^\infty(0,\mathsf{T};L^2(\Omega))$ in (5.15a) ensues from convergence results (5.22), while $\varrho \in C^0([0,\mathsf{T}];L^2(\Omega))$ is a consequence of the regularity in Bochner spaces for the Gelfand triple $V \Subset L^2(\Omega) \subset V^*$.

To 2. Assume that the initial datum satisfies $r_* \le \varrho_0 \le r^*$ a.e. in Ω. We observe that the functions $\max\{\varrho - r^*, 0\}|_{[0,t]}$ and $\min\{\varrho - r_*, 0\}|_{[0,t]}$ for all $t \in [0,\mathsf{T}]$ are admissible test functions for (5.15b) since they are compositions of Lipschitz-continuous functions with Sobolev functions, cf. [MM79]. Subsequent integration by parts in time results in the relations

$$
\begin{aligned}
0 &= \|\max\{\varrho(t) - r^*, 0\}\|^2_{L^2(\Omega)} - \|\max\{\varrho_0 - r^*, 0\}\|^2_{L^2(\Omega)} + \int_{Q_t \cap [\varrho \ge r^*]} \widehat{\mathrm{K}}(\varrho,\theta)\nabla\varrho\cdot\nabla\varrho \,\mathrm{d}x\,\mathrm{d}s\,,\\
0 &= \|\min\{\varrho(t) - r_*, 0\}\|^2_{L^2(\Omega)} - \|\min\{\varrho_0 - r_*, 0\}\|^2_{L^2(\Omega)} + \int_{Q_t \cap [\varrho \le r_*]} \widehat{\mathrm{K}}(\varrho,\theta)\nabla\varrho\cdot\nabla\varrho \,\mathrm{d}x\,\mathrm{d}s
\end{aligned}
$$

for any $t \in (0,\mathsf{T}]$. In both expressions, the second term is zero due to the boundedness of the initial datum. Moreover, in both expressions the third term is non-negative thanks to (5.13). Thus, necessarily $\max\{\varrho(t) - r^*, 0\} = \min\{\varrho(t) - r_*, 0\} = 0$ a.e. in Ω, which concludes the proof of statement 2. □

Remark 5.2 (Boundary conditions)**.** For simplicity we have formulated Thm. 5.1 with homogeneous Neumann boundary conditions $\widehat{\mathrm{K}}(\varrho(t),\theta)\nabla\varrho(t)\cdot\boldsymbol{n} = 0$ on $\partial\Omega$ for all $t \in [0,\mathsf{T}]$ with $\boldsymbol{n}$ the outer unit normal vector to $\partial\Omega$. This can be extended to inhomogeneous Neumann boundary conditions for a prescribed datum $h \in H^{-1/2}(\partial\Omega,\mathbb{R}^d)$, so that (5.15b) additionally features the term $\int_0^\mathsf{T}\int_{\partial\Omega} hv \,\mathrm{d}S\,\mathrm{d}t$. Introducing $\emptyset \neq \partial_\mathrm{D}\Omega \subset \partial\Omega$ as the Dirichlet boundary and $\partial_\mathrm{N}\Omega = \partial\Omega\backslash\partial_\mathrm{D}\Omega$, Thm. 5.1 can also be adapted to inhomogeneous Dirichlet boundary conditions on $\partial_\mathrm{D}\Omega$. For this, consider $g \in H^1(\Omega)$ an extension of the given Dirichlet datum into the domain Ω and replace ϱ in (5.15b) by the shifted function $\varrho + g$, where both ϱ and the test functions v are now chosen in $V_0 := \{u \in H^1(\Omega) \,|\, u = 0 \text{ on } \partial_\mathrm{D}\Omega\}$ in space. This setting even provides a unique weak solution. We note that also statement 2. can be adapted to the case of inhomogeneous Dirichlet conditions: Given $g_\mathrm{D} \in H^{1/2}(\partial_\mathrm{D}\Omega)$ such that $g_\mathrm{D} \in [r_*, r^*]$ a.e. on $\partial_\mathrm{D}\Omega$ and $g \in H^1(\Omega)$ an extension of g_D into Ω one observes that $\max\{\varrho + g - r^*, 0\} \in V_0$ and $\min\{\varrho + g - r_*, 0\} \in V_0$ are admissible test functions, so that the proof of 2. can be reproduced.

5.1.3 Perusal of assumptions (5.8) & (5.13) for thermodynamical rock data

In the following we validate the mathematical assumptions (5.8) and (5.13) with the thermodynamical rock data used in [PJP+17]. Figure 5 shows the total mass density $\varrho = \tilde{\varrho}(\pi)$ as a function of pressure π in its geologically relevant range of 0.8-2 GPa, see also Sec. 4.4. Fig. 5 confirms that $\tilde{\varrho}$ is a continuous and strictly monotone function of pressure π, hence bijective. Yet, it also turns out that the map suffers from a kink at $\pi = 1.2$ GPa, which hampers the assumption of continuous differentiability of $\tilde{\varrho}$ and its inverse $\tilde{\varrho}^{-1}$, cf. (5.8b). Indeed, this kink coincides with a phase transformation between antigorite and olivine as shown is Fig. 3 and in Fig. 4. It therefore also appears in the porosity $\phi = \tilde{\phi}(\pi,\theta)$ and in the coefficient function $\widetilde{\mathrm{K}}(\pi,\theta)$ at $\pi = 1.2$ GPa, see Fig. 6. As expected this translates into a discontinuity of the coefficient function $\widehat{\mathrm{K}}(\cdot,\theta)$ at $\varrho \approx 2600$ kg/m^3. We further point out that the porosity shown in Fig.6 is strictly positive and bounded from below by the value $\tilde{\phi}(2\text{GPa}, 480°\text{C}) = 0.035 > 0$. In turn, we find the coefficient function $\widehat{\mathrm{K}}(\cdot,\theta)$ to be uniformly bounded from above and from below by a value strictly larger than zero, so that assumption (5.13b) is satisfied.

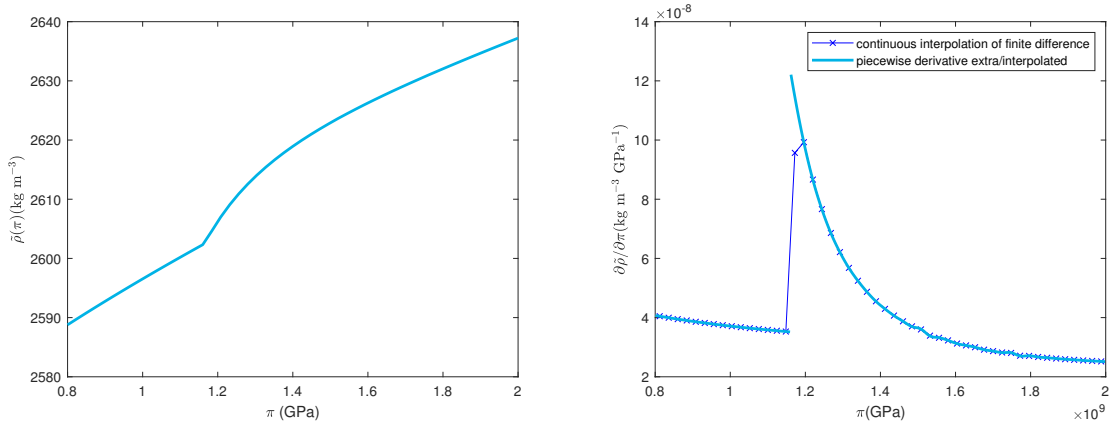

Figure 5: on the left: Example of $\tilde{\varrho} = \tilde{\varrho}(\pi, \theta)$ for a given composition and at fixed temperature of $480°$C. One can see the continuity and strict monotonicity of $\tilde{\varrho}$ which in return guarantee the existence of a continuous inverse $\tilde{\varrho}^{-1}$. On the right: plot of the derivative $\partial\tilde{\varrho}/\partial\pi$ for two possible discretizations. It can bee seen that it is discontinuous at $\pi = 1.2$GPa and that is bounded from below and above satisfying assumption (5.8c).

As the violation of the continuity assumptions (5.13a) for $\widehat{\mathrm{K}}(\cdot, \theta)$ and (5.8b) are concerned, we point out that the analytical results given in Thm. 5.1, 2. predict that the weak solution $\varrho(t, \cdot)$ for all $t \in [0, \mathsf{T}]$ stays confined between values $0 < r_* < r^*$ a.e. in Ω, if the initial datum ϱ_0 is chosen with this property. In other words, if the initial datum is chosen with values strictly below or strictly above the critical value of $\varrho = 2600$ kg/m^3 (corresponding to the critical pressure of 1.2 GPa), then also the solution will not exceed this value apart from a set of zero measure at any later time $t \in (0, \mathsf{T}]$. Thus, under this additional assumption on the initial datum, all the assumptions (5.8) and (5.13) are met and therefore existence of a unique weak solution is guaranteed by Thm. 5.1, 1. However, this also means that in this setting the phase transition, with ϱ exceeding the critical value on sets of positive measure, cannot be described by Thm. 5.1 using the original thermodynamical data set. Instead, in order to cover also this case, one would have to mollify $\tilde{\varrho}(\cdot, \theta)$ and $\widehat{\mathrm{K}}(\cdot, \theta)$ in a small neighbourhood of the non-smoothness. From a geological perspective, even though the interesting pressure range is between 0.8-2 GPa, it is very difficult for a geological system to experience this complete range. Usually, pressure variations are very small and π is confined to a neighborhood of a certain value. Therefore it is usually sufficient to study one of either areas below or above 1.2 GPa. Additionally let us point out that the phase stability, hence the position of the kink, varies with temperature and rock composition: If the system has a high iron content, one would find this kink in the mass density for higher values of pressure, cf. [HVJ22]. As explained in Fig. 3 for the composition and temperature of this specific example, antigorite, the hydrated rock, is stable for pressure values above 1.2 GPa and olivine, the dehydrated rock, is stable at pressure values below 1.2 GPa. In conclusion, since the interest lies in the investigation of the dehydration process, we can confine the analysis to the regime below 1.2 GPa.

5.2 Results and challenges of model (1.2)

Although the application of a similar approach as the one used in Section 5.1.2 might seem straightforward, the thermodynamical data behind the model (1.2) hide a series of challenges that require a special treatment. We dedicate this section to their description.

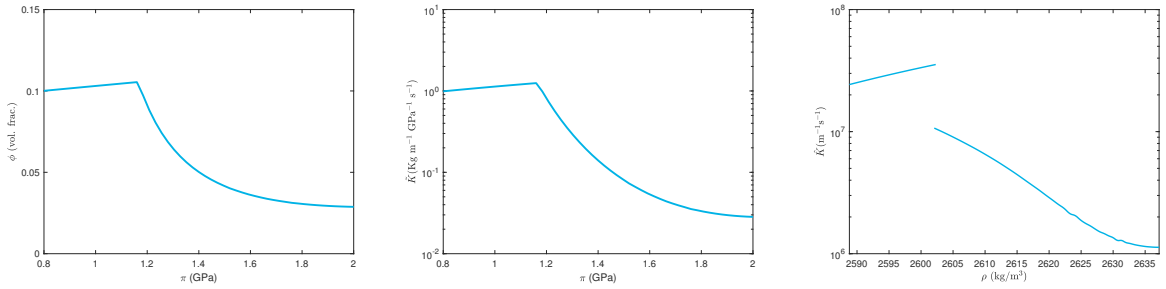

Figure 6: Example of $\phi = \phi(\pi, \theta)$, $\hat{K}(\pi, \theta)$ and $\tilde{K}(\pi, \theta)$ for a given composition and at fixed temperature of $480°$C. For these simulations we have set ratio between permeability of the medium and viscosity of the fluid $\hat{K}/\mu = 1$. Thus, positivity and continuity of $\hat{K}$ relies on ϕ, which never reaches zero.

5.2.1 Parabolic form of system (1.2)

Also in model (1.2) it is assumed that the quantities

$$\begin{aligned} &\varrho_{\mathrm{s}} = \tilde{\varrho}_{\mathrm{s}}(\pi, c_{\mathrm{s}}, \theta), \quad \varrho_{\mathrm{f}} = \tilde{\varrho}_{\mathrm{f}}(\pi, c_{\mathrm{s}}, \theta), \quad c_{\mathrm{f}} = \tilde{c}_{\mathrm{f}}(\pi, c_{\mathrm{s}}, \theta) \text{ are given functions} \\ &\text{of pressure } \pi, \text{ concentration } c_{\mathrm{s}}, \text{ and temperature } \theta\,. \end{aligned} \tag{5.23}$$

Again, their analytical form is unknown, but their values can be determined from thermodynamical data tables. Combining (5.23) and (1.2c) also the porosity ϕ can be understood as a function of the variables $(\pi, c_{\mathrm{s}}, \theta)$ as follows

$$\phi = 1 - \frac{\varrho_{\mathrm{s}}^0(1-c_{\mathrm{s}}^0-X_{\mathrm{h}}^0)(1-\phi^0)}{\tilde{\varrho}_{\mathrm{s}}(\pi,c_{\mathrm{s}},\theta)(1-\tilde{c}_{\mathrm{s}}-\tilde{X}_{\mathrm{h}}(\pi,c_{\mathrm{s}},\theta))} =: \tilde{\phi}(\pi, c_{\mathrm{s}}, \theta)\,. \tag{5.24}$$

Based on this we introduce the notation

$$\tilde{\varrho}_1(\pi, c_{\mathrm{s}}, \theta) := \tilde{\varrho}_{\mathrm{f}}(\pi, c_{\mathrm{s}}, \theta)\tilde{\phi}(\pi, c_{\mathrm{s}}, \theta) + \tilde{\varrho}_{\mathrm{s}}(\pi, c_{\mathrm{s}}, \theta)\big(1 - \tilde{\phi}(\pi, c_{\mathrm{s}}, \theta)\big)\,, \tag{5.25a}$$

$$\tilde{\varrho}_2(\pi, c_{\mathrm{s}}, \theta) := \tilde{\varrho}_{\mathrm{f}}(\pi, c_{\mathrm{s}}, \theta)\tilde{\phi}(\pi, c_{\mathrm{s}}, \theta)\tilde{c}_{\mathrm{f}}(\pi, c_{\mathrm{s}}, \theta) + \tilde{\varrho}_{\mathrm{s}}(\pi, c_{\mathrm{s}}, \theta)\big(1 - \tilde{\phi}(\pi, c_{\mathrm{s}}, \theta)\big)c_{\mathrm{s}}\,, \tag{5.25b}$$

$$\widetilde{\mathrm{K}}_1(\pi, c_{\mathrm{s}}, \theta) := \tilde{\varrho}_{\mathrm{f}}(\pi, c_{\mathrm{s}}, \theta)K_\phi(\tilde{\phi}(\pi, c_{\mathrm{s}}, \theta))\,, \tag{5.25c}$$

$$\widetilde{\mathrm{K}}_2(\pi, c_{\mathrm{s}}, \theta) := \tilde{\varrho}_{\mathrm{f}}(\pi, c_{\mathrm{s}}, \theta)\tilde{c}_{\mathrm{f}}(\pi, c_{\mathrm{s}}, \theta)K_\phi(\tilde{\phi}(\pi, c_{\mathrm{s}}, \theta))\,, \tag{5.25d}$$

$$K_\phi(\tilde{\phi}(\pi, c_{\mathrm{s}}, \theta)) := \frac{\kappa}{\mu}\tilde{\phi}(\pi, c_{\mathrm{s}}, \theta)^3\,, \tag{5.25e}$$

$$\widetilde{\mathbb{D}}(\pi, c_{\mathrm{s}}, \theta) := \tilde{\varrho}_{\mathrm{f}}(\pi, c_{\mathrm{s}}, \theta)\tilde{\phi}(\pi, c_{\mathrm{s}}, \theta)D_c\,, \tag{5.25f}$$

with constants $\kappa, \mu, D_c > 0$. Thus, equations (1.2a) and (1.2b) can be rewritten as follows

$$\partial_t\tilde{\varrho}_1(\pi, c_{\mathrm{s}}, \theta) = \nabla \cdot \Big(\widetilde{\mathrm{K}}_1(\pi, c_{\mathrm{s}}, \theta)\nabla\pi\Big)\,, \tag{5.26a}$$

$$\partial_t\tilde{\varrho}_2(\pi, c_{\mathrm{s}}, \theta) = \nabla \cdot \Big(\widetilde{\mathrm{K}}_2(\pi, c_{\mathrm{s}}, \theta)\nabla\pi + \widetilde{\mathbb{D}}(\pi, c_{\mathrm{s}}, \theta)\nabla\tilde{c}_{\mathrm{f}}(\pi, c_{\mathrm{s}}, \theta)\Big)\,. \tag{5.26b}$$

This is a PDE system of the form

$$\partial_t\tilde{\boldsymbol{\varrho}}(\boldsymbol{q}, \theta) - \nabla \cdot \Big(\widetilde{\mathrm{K}}_{\mathrm{D}}(\boldsymbol{q}, \theta)\nabla\boldsymbol{q}\Big) = 0 \quad \text{with} \tag{5.27a}$$

$$\boldsymbol{q} := \begin{pmatrix}\pi\\ c_{\mathrm{s}}\end{pmatrix}\,, \quad \tilde{\boldsymbol{\varrho}} := \begin{pmatrix}\tilde{\varrho}_1\\ \tilde{\varrho}_2\end{pmatrix}\,, \quad \widetilde{\mathrm{K}}_{\mathrm{D}} := \begin{pmatrix}\widetilde{\mathrm{K}}_1 & 0\\ \widetilde{\mathrm{K}}_2 + \partial_\pi\tilde{c}_{\mathrm{f}}\widetilde{\mathbb{D}} & \partial_{c_{\mathrm{s}}}\tilde{c}_{\mathrm{f}}\widetilde{\mathbb{D}}\end{pmatrix}\,, \tag{5.27b}$$

where we have used the chain rule $\nabla \tilde{c}_\mathrm{f} = \partial_\pi \tilde{c}_\mathrm{f} \nabla \pi + \partial_{c_\mathrm{s}} \tilde{c}_\mathrm{f} \nabla c_\mathrm{s}$. Now we set

$$\boldsymbol{\varrho} := \tilde{\boldsymbol{\varrho}}(\boldsymbol{q}, \theta) \tag{5.28}$$

and make the following assumptions on the map $\tilde{\boldsymbol{\varrho}}$ and its inverse

$$\begin{aligned} &\text{for every } \theta > 0 \text{ fixed the function } \tilde{\boldsymbol{\varrho}}(\cdot, \theta) \text{ is continuously differentiable in } \boldsymbol{q} \\ &\text{and invertible in } \boldsymbol{q} \text{ and the inverse} \\ &\tilde{\boldsymbol{\varrho}}^{-1}(\cdot, \theta) \text{ is continuously differentiable.} \end{aligned} \tag{5.29a}$$

We note that assumptions (5.29) amount to the following conditions

$$\text{For all } \theta > 0 \text{ the Jacobian } \mathrm{D}_{\boldsymbol{q}} \tilde{\boldsymbol{\varrho}}(\cdot, \theta) = \begin{pmatrix} \partial_\pi \tilde{\varrho}_1(\cdot, \theta) & \partial_{c_\mathrm{s}} \tilde{\varrho}_1(\cdot, \theta) \\ \partial_\pi \tilde{\varrho}_2(\cdot, \theta) & \partial_{c_\mathrm{s}} \tilde{\varrho}_2(\cdot, \theta) \end{pmatrix} \text{ is continuous with} \tag{5.30a}$$

$$\det \mathrm{D}_{\boldsymbol{q}} \tilde{\boldsymbol{\varrho}}(\boldsymbol{q}, \theta) > 0 \text{ for all admissible } \boldsymbol{q} \in \mathbb{R}^2 \text{, and also} \tag{5.30b}$$

$$\mathrm{D}_{\boldsymbol{\varrho}} \tilde{\boldsymbol{\varrho}}^{-1}(\cdot, \theta) = \mathrm{D}_{\boldsymbol{q}} \tilde{\boldsymbol{\varrho}}(\tilde{\boldsymbol{\varrho}}^{-1}(\cdot, \theta), \theta)^{-1} \text{ is a continuous function in } \boldsymbol{\varrho}\,. \tag{5.30c}$$

Then we have

$$\boldsymbol{q} = \tilde{\boldsymbol{\varrho}}^{-1}(\boldsymbol{\varrho}, \theta) =: \tilde{\boldsymbol{q}}(\boldsymbol{\varrho}, \theta) \tag{5.31}$$

and system (5.27) can be rewritten as a parabolic PDE system of the form

$$\partial_t \boldsymbol{\varrho} - \nabla \cdot \left(\widehat{\mathrm{K}}_\mathrm{D}(\boldsymbol{\varrho}, \theta) \nabla \boldsymbol{\varrho} \right) = 0\,, \tag{5.32a}$$

where we used the relations

$$\nabla \boldsymbol{q} = \partial_{\boldsymbol{\varrho}} \tilde{\boldsymbol{q}}(\boldsymbol{\varrho}, \theta) \nabla \boldsymbol{\varrho} \quad \text{and} \quad \widehat{\mathrm{K}}_\mathrm{D}(\boldsymbol{\varrho}, \theta) := \widetilde{\mathrm{K}}_\mathrm{D}(\tilde{\boldsymbol{q}}(\boldsymbol{\varrho}, \theta), \theta) \partial_{\boldsymbol{\varrho}} \tilde{\boldsymbol{q}}(\boldsymbol{\varrho}, \theta)\,. \tag{5.32b}$$

We now state the following assumptions on $\widehat{\mathrm{K}}_\mathrm{D}$:

For all $\theta > 0$ the matrix $\widehat{\mathrm{K}}_\mathrm{D}(\cdot, \theta)$ has the following properties:

- $\widehat{\mathrm{K}}_\mathrm{D}(\cdot, \theta) : \mathbb{R}^2 \to \mathbb{R}^{2\times 2}$ is continuous, (5.33a)
- $\widehat{\mathrm{K}}_\mathrm{D}(\boldsymbol{q}, \theta) : \mathbb{R}^{2\times 2} \to \mathbb{R}^{2\times 2}$ is bounded and positively definite uniformly wrt. $(\boldsymbol{q}, \theta)$, (5.33b)
  i.e., there are constants $0 < K_* < K^*$ s.th. for all $(\boldsymbol{q}, \theta)$ and all $\boldsymbol{v} \in \mathbb{R}^2$ there holds :
  $$K_* |\boldsymbol{v}|^2 \leq \boldsymbol{v} \cdot \widehat{\mathrm{K}}_\mathrm{D}(\boldsymbol{q}, \theta) \boldsymbol{v} \leq K^* |\boldsymbol{v}|^2\,.$$

5.2.2 Existence of weak solutions

We observe that assumptions (5.30) and (5.33) are the immediate translation of the assumptions from the scalar-valued to the vector-valued setting. Accordingly, we here state the following existence result. Its proof closely follows the outline given in Section 5.1.2 and we refer the reader to [ZT23, Sec. 3, 4] for further details.

Theorem 5.3 (Existence of a weak solution for system (5.32))**.** *Let the prerequisites of Theorem 5.1 be satisfied and denote* $\boldsymbol{V} := V \times V$*. Then the following statements hold true:*

1 *Let* $\boldsymbol{\varrho_0} \in \boldsymbol{V}$ *be a given initial datum and assume that* $\widehat{\mathrm{K}}_\mathrm{D}(\cdot, \theta)$ *satisfies* (5.33)*. Then there exists a function*

$$\boldsymbol{\varrho} \in H^1(0, \mathsf{T}; \boldsymbol{V}^*) \cap L^2(0, \mathsf{T}; \boldsymbol{V}) \cap L^\infty(0, \mathsf{T}; L^2(\Omega, \mathbb{R}^2)) \cap C^0([0, \mathsf{T}]; L^2(\Omega; \mathbb{R}^2))\,, \tag{5.34a}$$

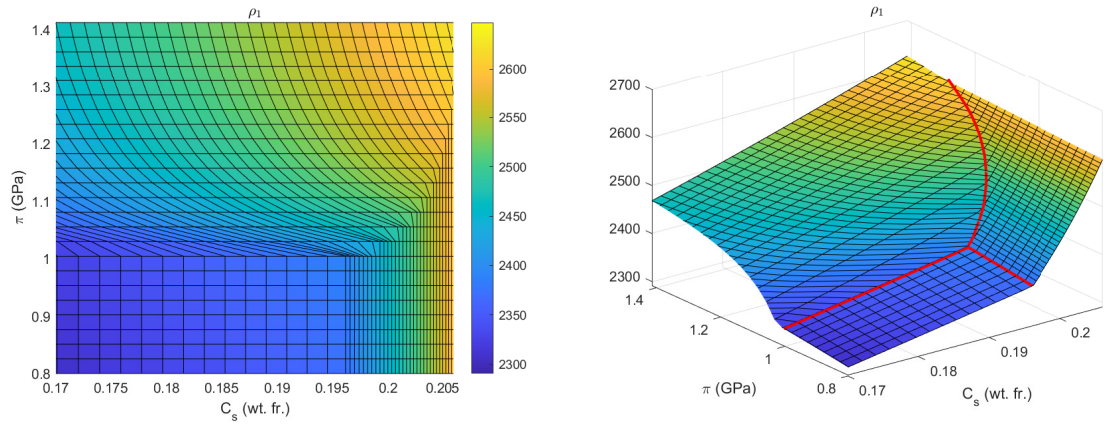

Figure 7: Plots of the total mass density $\tilde{\varrho}_1 = \tilde{\varrho}_1(\pi, c_\mathrm{s}, \theta)$. On the left a 2D plot showing the discretization grid resulting from an interpolation of the thermodynamic dataset. The non-differentiability points are marked with a red line in the right plot. This shows the division into three main areas ($(0.8, 1)$GPa $\times$ $(0.17, 0.196)$, $(0.8, 1)$GPa $\times$ $(0.196, 0.2)$ and the remaining part of the domain) delimited by two straight lines and one curve with a contact point around $(1\text{GPa}, 0.195)$. These three subdivisions and the values for which $\tilde{\varrho}_1$ is continuous but not differentiable are more clearly seen in the 3D plot on the right.

which satisfies

$$\int_{Q_\mathsf{T}} \Big(\partial_t \boldsymbol{\varrho} \cdot \boldsymbol{v} + \widehat{\mathrm{K}}_\mathrm{D}(\boldsymbol{\varrho}, \theta) \nabla \boldsymbol{\varrho} : \nabla \boldsymbol{v} \Big) \,\mathrm{d}x \,\mathrm{d}t = 0 \quad \textit{for all } \boldsymbol{v} \in L^2(0, \mathsf{T}; \boldsymbol{V}). \tag{5.34b}$$

and $\boldsymbol{\varrho}(0) = \boldsymbol{\varrho_0}$.

2 *Further assume that there are constants* $0 < r_{1*} < r_1^*$ *and* $0 < r_{2*} < r_2^*$ *such that* $r_{1*} \leq \varrho_{10}(x) \leq r_1^*$ *as well as* $r_{2*} \leq \varrho_{20}(x) \leq r_2^*$ *holds true for a.e.* $x \in \Omega$ *for the initial datum* $\boldsymbol{\varrho_0} = (\varrho_{10}, \varrho_{20})^\top$. *Then for all* $t \in [0, \mathsf{T}]$ *also a solution* $\boldsymbol{\varrho} = (\varrho_1, \varrho_2)^\top$ *satisfies* $r_{1*} \leq \varrho_1(t, x) \leq r_1^*$ *as well as* $r_{2*} \leq \varrho_2(t, x) \leq r_2^*$ *for a.e.* $x \in \Omega$.

5.2.3 Perusal of assumptions (5.30) & (5.33) for thermodynamical rock data

Firstly we recall that system (1.2) is written in terms of $\boldsymbol{q} = (\pi, c_\mathrm{s})^\top$, i.e., in terms of the pressure π and the concentration of silica in the solid c_s. A close inspection of the thermodynamical rock data sets reveals that the introduction of this additional complexity causes the resulting mass densities to have regions of non-invertibility and non-differentiability, as it can be seen in Figures 7 and 8 for the mass densities $\tilde{\varrho}_1$ and $\tilde{\varrho}_2$. This is in analogy to the kink in the thermodynamical data of model (1.1) shown in Fig. 6. More precisely, we see in Fig. 7 that the total mass density $\tilde{\varrho}_1$ is strictly monotonously increasing with respect to pressure and silica-content, but that kinks arise in the region of the antigorite-olivine phase transition discussed in Fig. 3. Similarly, also Fig. 8 shows a monotone behavior of the total silica-mass density $\tilde{\varrho}_2$ in pressure and silica-content, also with kinks arising at the antigorite-olivine phase transition. Obviously, within this region assumptions (5.29) and (5.30) are not satisfied.

Additionally we point out that in (1.2) the gradient of the silica concentration in the fluid $\tilde{c}_\mathrm{f}$ drives the diffusion process. Hence, it would be natural to chose $\tilde{c}_\mathrm{f}$ as a variable. However, as Fig. 9 reveals, in wide areas of the data range $\tilde{c}_\mathrm{f}$ is constant with respect to c_s, so that the function is not invertible in these areas. This is the reason why system (5.26) is written in terms of the variables π and c_s. Indeed, such plateau regions followed

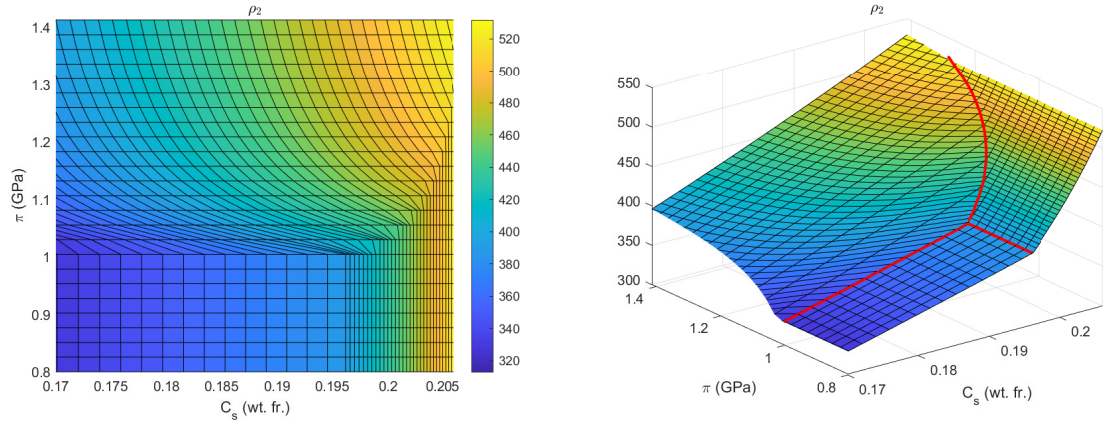

Figure 8: Plots of the total mass density of silica $\tilde{\varrho}_2 = \tilde{\varrho}_2(\pi, c_\mathrm{s}, \theta)$. On the left a 2D plot showing the discretization grid resulting from an interpolation of the thermodynamic dataset. The non-differentiability points are marked with a red line in the right plot. This shows the division into three main areas (the same of $\tilde{\varrho}_1$ shown in Figure 7). These three subdivisions and the values for which $\tilde{\varrho}_2$ is continuous but not differentiable are more clearly seen in the 3D plot on the right.

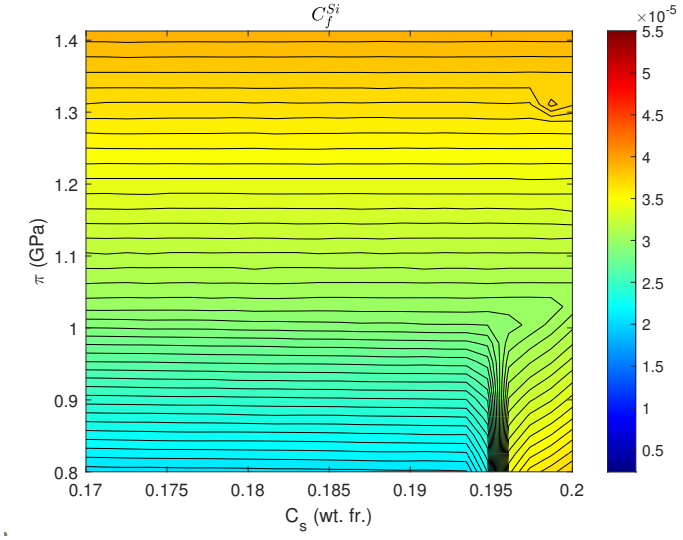

Figure 9: The figure shows isolevels for the function $\tilde{c}_\mathrm{f}(\pi, \tilde{c}_\mathrm{s})$ at $\theta = 480°$C. One can see that in most parts of the considered domain we have $\partial c_\mathrm{f}/\partial c_\mathrm{s} = 0$ which translates to no diffusion occurring in the system. However it is worth noticing that there is a small area in the bottom right corner where this condition is not met. In addition, a discontinuity point where the lines are more dense can be seen around $c_\mathrm{s} \approx 0.195$. This discontinuity would, i.e., invalidates assumption (5.33a)

by kinks as in Fig. 9 are common in thermodynamical rock data sets. They are also predicted in [Guy93] in the case of non-convex thermodynamical functions, which is again closely related to phase stability.

As can be seen from (5.27), in regions where $\partial \tilde{c}_\mathrm{f}/\partial c_\mathrm{s} = 0$, diffusion of silica is absent and the mathematical classification of the PDE system becomes unclear. Similar to Section 5.1.3 one may also try here to confine the initial data to a data range that ensures the validity of assumptions (5.30) and (5.33). Then the results of Theorem

5.3 would also guarantee that solutions are confined to that data range for all times $t \in (0, T]$. However, as can be seen from (5.27) the positive definiteness of $\widehat{\mathrm{K}}_{\mathrm{D}}$, and hence the classification of the PDE system, is not solely linked to the positive definiteness of the Jacobian $\mathrm{D}_{\boldsymbol{q}\tilde{\boldsymbol{\varrho}}}$ but also to the values of the material constants κ, μ, and D_{c} contributing to the non-symmetric coefficient matrix $\widetilde{\mathrm{K}}$ in (5.27). These material constants are, in fact, the main contributors, together with $\partial\tilde{c}_{\mathrm{f}}/\partial c_{\mathrm{s}}$ and $\partial\tilde{c}_{\mathrm{f}}/\partial\pi$, to the parabolicity of the system. In the literature, see e.g. [WW97], it is discussed that potential values for D_c and μ range from 10^{-8}-$10^{-10}\mathrm{m}^2/\mathrm{s}$ and 10^{-4}Pa·s while for the permeability κ one finds 10^{-17}-$10^{-14}\mathrm{m}^2$, see e.g. [MI99]. An unprecise tuning of the system might lead to fail the assumption (5.33b). This is exemplary seen in Figure 10, where we have plotted the eigenvalues of $\mathrm{sym}\hat{K} = 1/2(\hat{K} + \hat{K}^\top)$. In the considered range of pressure and concentration it turns out that its smallest eigenvalue is negative whereas the largest eigenvalue is positive. In fact, the uniform positive definiteness of $\widehat{\mathrm{K}}$, i.e., a lower bound as in (5.33b), is equivalent to $\mathrm{sym}\hat{K}$ being positive definite.

As a further difficulty it turns out that the computation of the thermodynamical data set is highly sensitive to the total composition and therefore to the function $\tilde{c}_{\mathrm{f}}$. This creates approximation errors in the plateau region where $\partial\tilde{c}_{\mathrm{f}}/\partial c_{\mathrm{s}} = 0$ that may cause backward diffusion in the system.

Different strategies can be deployed to circumvent this problem: the interpolation of the approximated $\tilde{c}_{\mathrm{f}}$ function could be constructed to ensure that $\partial\tilde{c}_{\mathrm{f}}/\partial c_{\mathrm{s}} = 0 > \delta > 0$. Alternatively, more sophisticated and invasive solutions rely on extensions of the system that account for further geophysical phenomena that could help mitigate this behavior. One possibility is to include more species and phases, which would lead to a change in the landscape of $\tilde{c}_{\mathrm{f}}$, possibly avoiding a plateau of the previous type. In general, non-convex regions in the energy landscape can produce $\partial\tilde{c}_{\mathrm{f}}/\partial c_{\mathrm{s}} = 0$ of different signs, indicating that phase separation is taking place. In such a case, higher-order derivatives as in the Cahn-Hilliard model might help to ensure the mathematical well-posedness of the problem.

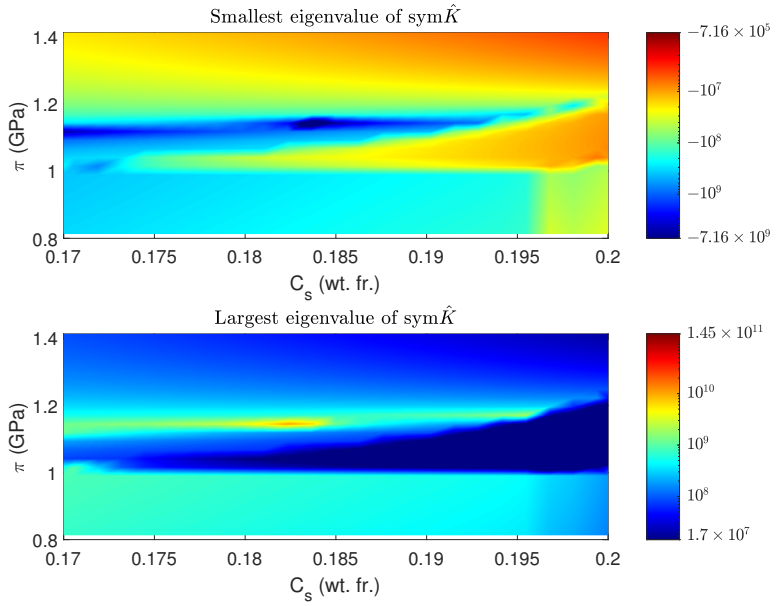

Figure 10: The figure shows the eigenvalue for the symmetrized operator $\mathrm{sym}\hat{K} = 1/2(\hat{K} + \hat{K}^\top)$ for $\theta = 480°$C. For the considered range of pressure and concentration the smallest eigenvalue is well kept below 0 while the largest is clearly positive.

References

[ADDN04] Denise Aregba-Driollet, Fasma Diele, and Roberto Natalini. A mathematical model for the sulphur dioxide aggression to calcium carbonate stones: Numerical approximation and asymptotic analysis. *SIAM Journal on Applied Mathematics*, 64(5):1636–1667, 2004.

[APDH+14] Samuel Angiboust, Thomas Pettke, Jan C.M. De Hoog, Benoit Caron, and Onno Oncken. Channelized Fluid Flow and Eclogite-facies Metasomatism along the Subduction Shear Zone. *J. Petrol.*, 55(5):883–916, 2014.

[BA02] Christopher M. Breeding and Jay J. Ague. Slab-derived fluids and quartz-vein formation in an accretionary prism, Otago Schist, New Zealand. *Geology*, 30(6):499 – 502, 2002.

[BJK+18] Wasja Bloch, Timm John, Jörn Kummerow, Pablo Salazar, Oliver S. Krüger, and Serge A Shapiro. Watching dehydration: Seismic Indication for Transient Fluid Pathways in the Oceanic Mantle of the Subducting Nazca Slab. *Geochem. Geophys. Geosyst.*, 19(9):3189–3207, 2018.

[BJV+20] Andreas Beinlich, Timm John, Johannes C. Vrijmoed, Masako Tominaga, Tomas Magna, and Yuri Y. Podladchikov. Instantaneous rock transformations in the deep crust driven by reactive fluid flow. *Nat. Geosci.*, 13(4):307–311, 2020.

[BPL82] Lee E. Baker, Alan C. Pierce, and Kraemer D. Luks. Gibbs energy analysis of phase equilibria. *Society of Petroleum Engineers Journal*, 22(05):731–742, 1982.

[CHJ+19] Shuo Chen, Remco C. Hin, Timm John, Richard Brooker, Ben Bryan, Yaoling Niu, and Tim Elliott. Molybdenum systematics of subducted crust record reactive fluid flow from underlying slab serpentine dehydration. *Nat. Commun.*, 10, 4773, 2019.

[Con17] James A.D. Connolly. A primer in gibbs energy minimization for geophysicists. *Petrology*, 25(5):526–534, 2017.

[Cou04] Olivier Coussy. *Poromechanics*. John Wiley & Sons, 2004.

[CPNT19] Maxime Clément, José Alberto Padrón-Navarta, and Andréa Tommasi. Interplay between fluid extraction mechanisms and antigorite dehydration reactions (Val Malenco, Italian Alps). *J. Petrol.*, 60(10):1935–1962, 2019.

[DJ12] Michael Dreher and Ansgar Jüngel. Compact families of piecewise constant functions in $L^p(0,T;B)$. *Nonlinear Analysis: Theory, Methods & Applications*, 75(6):3072 – 3077, 2012.

[Ehl09] Wolfgang Ehlers. Challenges of porous media models in geo-and biomechanical engineering including electro-chemically active polymers and gels. *International Journal of Advances in Engineering Sciences and Applied Mathematics*, 1(1):1–24, 2009.

[Flo42] Paul J. Flory. Thermodynamics of high polymer solutions. *The Journal of Chemical Physics*, 10(1):51–61, 1942.

[GÖ97] Miroslav Grmela and Hans Christian Öttinger. Dynamics and thermodynamics of complex fluids. I. Development of a general formalism. *Phys. Rev. E*, 56(6):6620–6632, 1997.

[Guy93] Bernard Guy. Mathematical revision of Korzhinskii's theory of infiltration metasomatic zoning. *Eur. J. Mineral.*, 5:317–339, 1993.

[HJBS12] Petra Herms, Timm John, Ronald J. Bakker, and Volker Schenk. Evidence for channelized external fluid flow and element transfer in subducting slabs (Raspas Complex, Ecuador). *Chemical Geology*, 310-311:79–96, 2012.

[Hug41] Maurice L. Huggins. Solutions of long chain compounds. *The Journal of Chemical Physics*, 9(5):440–440, 1941.

[HVJ22] Konstantin Huber, Johannes C. Vrijmoed, and Timm John. Formation of olivine veins by reactive fluid flow in a dehydrating serpentinite. *Geochemistry, Geophysics, Geosystems*, 23(6):e2021GC010267, 2022.

[JGP+12] Timm John, Nikolaus Gussone, Yuri Y. Podladchikov, Gray E. Bebout, Ralf Dohmen, Ralf Halama, Reiner Klemd, Tomas Magna, and Hans-Michael Seitz. Volcanic arcs fed by rapid pulsed fluid flow through subducting slabs. *Nat. Geosci.*, 5(7):489–492, 2012.

[JKGGS08] Timm John, Reiner Klemd, Jun Gao, and Carl-Dieter Garbe-Schoenberg. Trace-element mobilization in slabs due to non steady-state fluid-rock interaction: Constraints from an eclogite-facies transport vein in blueschist (Tianshan, China). *LITHOS*, 103(1-2):1–24, 2008.

[KP06] Pertti Koukkari and Risto Pajarre. Calculation of constrained equilibria by gibbs energy minimization. *Calphad*, 30(1):18–26, 2006.

[Kra14] Robert Friedrich Krause. Growth, modelling and remodelling of biological tissue, 2014.

[MI99] Craig E. Manning and Steven E. Ingebritsen. Permeability of the continental crust: Implications of geothermal data and metamorphic systems. *Reviews of Geophysics*, 37(1):127–150, 1999.

[Mie11] Alexander Mielke. A gradient structure for reaction-diffusion systems and for energy-drift-diffusion systems. *Nonlinearity*, 24(4):1329–1346, 2011.

[MM79] Moshe Marcus and Victor J. Mizel. Every superposition operator mapping one Sobolev space into another is continuous. *J. Functional Analysis*, 33:217–229, 1979.

[MPS21] Alexander Mielke, Mark A. Peletier, and Artur Stephan. EDP-convergence for nonlinear fast–slow reaction systems with detailed balance. *Nonlinearity*, 34(8):5762, 2021.

[MR13] Alexander Mielke and Eduard Rohan. Homogenization of elastic waves in fluid-saturated porous media using the Biot model. *Math. Models Methods Appl. Sci.*, 23(5):873–916, 2013.

[MR15] Alexander Mielke and Thomáš Roubíček. *Rate-independent Systems: Theory and Application*, volume 193 of *Applied Mathematical Sciences*. Springer, New York, 2015.

[ÖG97] Hans Christian Öttinger and Miroslav Grmela. Dynamics and thermodynamics of complex fluids. II. Illustrations of a general formalism. *Phys. Rev. E*, 56(6):6633–6655, 1997.

[OSC15] Vít Orava, Ondřej Souček, and Peter Cendula. Multi-phase modeling of non-isothermal reactive flow in fluidized bed reactors. *J. Comput. Appl. Math.*, 289:282–295, 2015.

[PJP+17] Oliver Plümper, Timm John, Yuri Y. Podladchikov, Johannes C. Vrijmoed, and Marco Scambelluri. Fluid escape from subduction zones controlled by channel-forming reactive porosity. *Nat. Geosci.*, 10(2):150–156, 2017.

[PNTG+10] Jose Alberto Padrón-Navarta, Andrea Tommasi, Carlos J. Garrido, Vicente Lopez Sanchez-Vizcaino, Maria Teresa Gomez-Pugnaire, Antonio Jabaloy, and Alain Vauchez. Fluid transfer into the wedge controlled by high-pressure hydrofracturing in the cold top-slab mantle. *Earth Planet. Sci. Lett.*, 297(1–2):271–286, 2010.

[RMHC04] Lars H. Rüpke, Jason Phipps Morgan, Matthias Hort, and James A.D. Connolly. Serpentine and the subduction zone water cycle. *Earth and Planetary Science Letters*, 223(1):17–34, 2004.

[SPR11] Carl Spandler, Thomas Pettke, and Daniela Rubatto. Internal and External Fluid Sources for Eclogite-facies Veins in the Monviso Meta-ophiolite, Western Alps: Implications for Fluid Flow in Subduction Zones. *J. Petrol.*, 52(6):1207 – 1236, 2011.

[SvKA10] Ellen M. Syracuse, Peter E. van Keken, and Geoffrey A. Abers. The global range of subduction zone thermal models. *Physics of the Earth and Planetary Interiors*, 183(1-2):73–90, 2010.

[TJB+18] Stephan Taetz, Timm John, Michael Bröcker, Carl Spandler, and Andreas Stracke. Fast intraslab fluid-flow events linked to pulses of high pore fluid pressure at the subducted plate interface. *Earth Planet. Sci. Lett.*, 482:33–43, 2018.

[vKHSA11] Peter E. van Keken, Bradley R. Hacker, Ellen M Syracuse, and Geoff A Abers. Subduction factory: 4. Depth-dependent flux of H2O from subducting slabs worldwide. *J. Geophys. Res.*, 116:B01401, 2011.

[WW97] E. Bruce Watson and David A. Wark. Diffusion of dissolved sio2 in h2o at 1 gpa, with implications for mass transport in the crust and upper mantle. *Contributions to Mineralogy and Petrology*, 130(1):66–80, 1997.

[Zei86] Eberhard Zeidler. *Nonlinear Functional Analysis and its Applications I: Fixed-Point Theorems*. Springer-Verlag New York, 1986.

[ZPT21] Andrea Zafferi, Dirk Peschka, and Marita Thomas. Generic framework for reactive fluid flows. *ZAMM-Journal of Applied Mathematics and Mechanics/Zeitschrift für Angewandte Mathematik und Mechanik*, page e202100254, 2021.

[ZT23] Andrea Zafferi and Marita Thomas. Mathematical analysis of a porous-media model for rock-dehydration processes. Preprint, `https://www.wias-berlin.de/projects/sfb1114-c9/publication/mathematical_analysis_of_a_porous-media_model_for_rock-dehydration_processes.pdf`, 2023.